(2)

GL-TR-90-0260

Application of Regional Arrays in Seismic Verification Research

S. Mykkeltveit
F. Ringdal
T. Kvaerna
R. W. Alewine

NTNF/NORSAR
Post Box 51
N-2007 Kjeller, NORWAY

31 August 1990

Scientific Report No. 6

GEOPHYSICS LABORATORY
AIR FORCE SYSTEMS COMMAND
UNITED STATES AIR FORCE
HANSCOM AIR FORCE BASE, MASSACHUSETTS 01731-5000

Unclassified
SECURITY CLASSIFICATION OF THIS PAGE

REPORT DOCUMENTATION PAGE

Form Approved
OMB No. 0704-0188

1a. REPORT SECURITY CLASSIFICATION Unclassified	1b. RESTRICTIVE MARKINGS
2a. SECURITY CLASSIFICATION AUTHORITY	3. DISTRIBUTION/AVAILABILITY OF REPORT Approved for public release; Distribution unlimited
2b. DECLASSIFICATION/DOWNGRADING SCHEDULE	
4. PERFORMING ORGANIZATION REPORT NUMBER(S)	5. MONITORING ORGANIZATION REPORT NUMBER(S) GL-TR-90-0260
6a. NAME OF PERFORMING ORGANIZATION NTNF/NORSAR 6b. OFFICE SYMBOL (If applicable)	7a. NAME OF MONITORING ORGANIZATION Geophysics Laboratory
6c. ADDRESS (City, State, and ZIP Code) Post Box 51 N-2007 Kjeller, Norway	7b. ADDRESS (City, State, and ZIP Code) Hanscom Air Force Base Massachusetts 01731-5000
8a. NAME OF FUNDING/SPONSORING ORGANIZATION Defence Advanced Research Projects Agency 8b. OFFICE SYMBOL (If applicable) NMRO	9. PROCUREMENT INSTRUMENT IDENTIFICATION NUMBER Contract No. F49620-89-C-0038
8c. ADDRESS (City, State, and ZIP Code) 1400 Wilson Blvd. Arlington, VA 22209-2308	10. SOURCE OF FUNDING NUMBERS PROGRAM ELEMENT NO.: 62714E PROJECT NO.: 9A10 TASK NO.: DA WORK UNIT ACCESSION NO.: BH
11. TITLE (Include Security Classification) Application of Regional Arrays in Seismic Verification Research	
12. PERSONAL AUTHOR(S) S. Mykkeltveit, F. Ringdal, T. Kværna and R.W. Alewine	
13a. TYPE OF REPORT SCIENTIFIC REP. #6 13b. TIME COVERED FROM 90/05/01 TO 90/07/31	14. DATE OF REPORT (Year, Month, Day) 1990 August 31 15. PAGE COUNT 64
16. SUPPLEMENTARY NOTATION	

17. COSATI CODES			18. SUBJECT TERMS (Continue on reverse if necessary and identify by block number)
FIELD	GROUP	SUB-GROUP	Regional arrays, array design, NORESS and ARCESS arrays, array performance, network of arrays, seismic verification research. (JA?)

19. ABSTRACT (Continue on reverse if necessary and identify by block number)

The paper gives an account of the work related to the development of the NORESS concept of a regional array. The array design considerations and objectives are reviewed, and a description is given of the NORESS and ARCESS array facilities in Norway with their field installations, data transmission lines and data receiving center functions. The automatic signal detection processing of NORESS data applies multiple narrow-band frequency filters in parallel and forms array beams from selected subgeometries. The detection algorithm is based on computing the STA/LTA ratio for each beam individually, and a detection is declared whenever this ratio exceeds and given threshold. It is explained how the beam deployment and the individual threshold values can be tuned to ensure that the interesting phase arrivals are not missed, but at the same time avoiding coda detections. Keywords:

20. DISTRIBUTION/AVAILABILITY OF ABSTRACT ☐ UNCLASSIFIED/UNLIMITED ☐ SAME AS RPT. ☐ DTIC USERS	21. ABSTRACT SECURITY CLASSIFICATION UNCLASSIFIED
22a. NAME OF RESPONSIBLE INDIVIDUAL James Lewkowicz	22b. TELEPHONE (Include Area Code) (617) 377-3028 22c. OFFICE SYMBOL GL/LWH

DD Form 1473, JUN 86 *Previous editions are obsolete.* SECURITY CLASSIFICATION OF THIS PAGE

UNCLASSIFIED

19. (cont.)

For each detected signal, frequency-wavenumber analysis is invoked to determine arrival azimuth and apparent velocity. Currently, a broad band estimator is used, and it is demonstrated that use of this algorithm increases the stability of the azimuth and apparent velocity estimates, relative to narrow band methods. Local and regional events are automatically located on the basis of identification and association of P- and S-wa arrivals. The uncertainty in the arrival azimuth is the limiting factor in accurately determining single-array event locations, and it is shown that this uncertainty is as large as 10^{o}-15^{o} for Pn phases from certain regions.

In order to further investigate the potential of the NORESS concept, work was initiated towards installing a network of regional arrays in the northern Europe area. This involved the deployment of the ARCESS array in northern Norway, and the installation of the FINESA array in Finland in cooperation with the University of Helsinki. Data from these three arrays have been used jointly in a location estimation scheme. It is shown that for events in the Fennoscandian region of magnitude typically around 2.5 and for which at least one phase is detected by each array, location estimates can be obtained automatically that deviate from published network locations by only 16 km on the averag

In the future, it is anticipated that additional arrays and single stations in the northern Europe area will contribute real-time data to NORSAR for analysis jointly with existing arrays. The first additional data to become available will be from the GERESS array, which will be established in the Federal Republic of Germany in 1990. Future perspectives also include the use of expert system technology in the data analysis, and the IMS system already in operation represents the initial attempt in this regard. A summary is given of problem areas where further work is needed in order to fully exploi the regional array concept.

Preface

Under Contract No. F49620-C-89-0038, NTNF/NORSAR is conducting research within a wide range of subjects relevant to seismic monitoring. The emphasis of the research program is on developing and assessing methods for processing of data recorded by networks of small-aperture arrays and 3-component stations, for events both at regional and teleseismic distances. In addition, more general seismological research topics are addressed.

Each quarterly technical report under this contract presents one or several separate investigations addressing specific problems within the scope of the statement of work. Summaries of the research efforts within the program as a whole are given in annual technical reports.

This Scientific Report No. 6 presents a manuscript entitled "Application of Regional Arrays in Seismic Verification", by S. Mykkeltveit, F. Ringdal, T. Kværna and R.W. Alewine.

NORSAR Contribution No. 418

Accession For	
NTIS GRA&I	☒
DTIC TAB	☐
Unannounced	☐
Justification	
By	
Distribution/	
Availability Codes	
Dist	Avail and/or Special
A-1	

CONTENTS

Application of Regional Arrays in Seismic Verification Research

SVEIN MYKKELTVEIT*, FRODE RINGDAL*, TORMOD KVÆRNA* AND
RALPH W. ALEWINE**

* NTNF/NORSAR, P.O. Box 51, N-2007 Kjeller, Norway

** DARPA/NMRO, 1400 Wilson Blvd., Arlington, Virginia 22209, USA

ABSTRACT

The paper gives an account of the work related to the development of the NORESS concept of a regional array. The array design considerations and objectives are reviewed, and a description is given of the NORESS and ARCESS array facilities in Norway with their field installations, data transmission lines and data receiving center functions.

The automatic signal detection processing of NORESS data applies multiple narrow-band frequency filters in parallel and forms array beams from selected subgeometries. The detection algorithm is based on computing the STA/LTA ratio for each beam individually, and a detection is declared whenever this ratio exceeds a given threshold. It is explained how the beam deployment and the individual threshold values can be tuned to ensure that the interesting phase arrivals are not missed, but at the same time avoiding coda detections.

For each detected signal, frequency-wavenumber analysis is invoked to determine arrival azimuth and apparent velocity. Currently, a broad band estimator is used, and it is demonstrated that use of this algorithm increases the stability of the azimuth and apparent velocity estimates, relative to narrow band methods. Local and regional events are automatically located on the basis of identification and association of P- and S-wave arrivals. The uncertainty in the arrival azimuth is the limiting factor in accurately determining single-array event locations, and it is shown that this uncertainty is as large as 10°–15° for Pn phases from certain regions.

In order to futher investigate the potential of the NORESS concept, work was initiated towards installing a network of regional arrays in the northern Europe area. This involved the deployment of the ARCESS array in northern Norway, and the installation of the FINESA array in Finland in cooperation with the University of Helsinki. Data from these three arrays have been used jointly in a location estimation scheme. It is shown that for events in the Fennoscandian region of magnitude typically around 2.5 and for which at least one phase is detected by each array, location estimates can be obtained automatically that deviate from published network locations by only 16 km on the average.

In the future, it is anticipated that additional arrays and single stations in the northern Europe area will contribute real-time data to NORSAR for analysis jointly with existing arrays. The first additional data to become available will be from the GERESS array, which will be established in the Federal Republic of Germany in 1990. Future perspectives also include the use of expert system technology in the data analysis, and the IMS system already in operation represents the initial attempt in this regard. A summary is given of problem areas where further work is needed in order to fully exploit the regional array concept.

Introduction

The suggestion to use seismic arrays in order to detect, locate and identify low-magnitude events for the purpose of verifying compliance with nuclear testing treaties dates back to the Geneva Conference of experts in 1958. In the 1960s and 70s, seismic arrays were established in several countries around the world, and the arrays were generally designed for optimum detection capabilities for events at teleseismic distances. The most ambitious undertaking in this regard was the deployment of the LASA array in the United States (525 short period seismometers over an aperture of 200 km) and the NORSAR array in Norway (132 short period seismometers, array aperture 100 km). Over the years, operation of teleseismic arrays has testified to their excellent performance in detecting weak arrivals, as well as their ability to estimate the direction and apparent velocity of incoming signals. A detailed review of these developments is given by Ringdal

and Husebye (1982).

The trilateral negotiations during 1977–80 on a Comprehensive Test Ban Treaty prompted a shift of interest from observations made at teleseismic distances to wave propagation in the regional regime (up to 2–3000 km). It is in this context that experiments were initiated in Norway in 1979 towards the development of a "prototype" regional array, suitable for monitoring of low-level seismic activity within regional distance range. It was anticipated that this work would be aided and facilitated by the experience and knowledge gained from 10 years of operation of the NORSAR array, but it was also realized that new experimental data had to be obtained to adequately design an array with the desirable performance for regional seismic phases.

The purpose of this paper is both to offer an overview of the work conducted since 1979 relating to the development of the NORESS and ARCESS arrays, and at the same time to give an assessment of the capbilities of these arrays. The regional array program with its associated research activities from its inception in 1979 has grown to become significant in both size and diversity. A complete review of these developments is beyond the scope of this paper. We will instead focus upon those aspects of these developments that in our judgement are the most important ones in the seismic monitoring context. This is done by firstly reviewing the considerations that went into the NORESS design efforts, before details are given on the array installations and the NORESS and ARCESS field sites. The various steps in the automatic data processing are described, and the individual performance of each of the arrays in detecting and locating events at regional distances is assessed. Thereupon, we consider the capabilities of a network of NORESS-type arrays. In making our assessments, we summarize important findings available in the literature, and supplement these with hitherto unpublished results from our own recent research. Finally, the results obtained during these past ten years are discussed, and some perspectives for the future are given.

NORESS Design Considerations

The desirable characteristics of a prospective prototype regional array were formulated at the outset of the experiments initiated in 1979: The array should be designed for

optimum detection of regional seismic signals, and it should provide sufficient resolution to reliably estimate the apparent velocity and azimuth of all such signals. Furthermore, it was clear that the desirable performance of the array with respect to signal detection and characterization would need to be obtained over the wide range of frequencies typical of regional wave propagation. These requirements can be formulated in a more technical language, as follows:

- The array should provide close to optimum gain by beamforming for the phases and frequencies characteristic of regional wave propagation.
- The array geometry should be symmetric in order to offer equal capabilities for signals from all directions, and the response pattern should have a narrow main lobe and small side lobes.

It was clear at the outset that data from the NORSAR teleseismic array could not be used to infer an optimum array configuration for a regional array, as regional signals recorded at NORSAR with its minimum sensor separation of the order of 2.5 km are spatially aliased and furthermore do not correlate well even across the 10 km aperture subarrays. The main emphasis in the initial experiments was therefore placed on deriving signal and noise correlation curves for various frequency bands for intersensor separations in the distance interval 0–2 km. Such curves can be used to express the beamforming gain G via the formula:

$$G^2 = \sum_{i,j=1}^{N} C_{ij} \; / \; \sum_{i,j=1}^{N} \rho_{ij} \qquad (1)$$

where C_{ij} is the signal correlation between sensors i and j, ρ_{ij} is the corresponding noise correlation, and N is the number of sensors. The provisional configuration deployed in 1979 comprised only 6 instruments unevenly spaced within an aperture of 2 km. Still, signal and noise correlation curves were obtained that possessed most of the characteristic features and thus qualitatively resembled the curves derived later on from configurations comprising many more sensors. Examples of such curves, derived from the eventual 25-sensor NORESS geometry, are shown in Fig. 1.

Analytical representations of the very early versions of the signal and noise correlation curves were used by Mykkeltveit *et al* (1983) in equation (1) to find geometries that max-

imized the array gain G. It was demonstrated in that paper that optimized geometries could be obtained that were associated with theoretical gains well in excess of the standard $\sqrt{N}$ gain by utilizing negative minima in the observed noise correlation curves (see Fig. 1). Such optimum geometries, however, tended to be rather "peaked" in their frequency response, *i.e.*, a very high gain at one particular frequency was generally accompanied by low gains at other frequencies. The optimized geometries were characterized by one particular intersensor spacing being represented as many times as possible in the geometry. This distance reflected the separation for which the noise correlation curve attained its minimum, for a given frequency interval. For optimization explicitly taking several frequency bands into consideration (*e.g.*, by giving equal weight, in the gain expression, to each of five different frequency bands), again one single intermediate frequency dominated the geometry. At this stage, it was realized that it would be difficult to arrive at configurations with a sufficiently broad frequency response, following this strategy. Instead, the approach of estimating the gain via equation (1) was pursued in combination with design ideas set forth by Followill and Harris (1983). They proposed a geometry based on concentric rings spaced at log-periodic intervals in radius R, according to the relation:

$$R = R_{min} \cdot \alpha^n, \qquad n = 0, 1, 2, 3 \tag{2}$$

The geometry of the NORESS array deployed in 1984 is a realization of (2), with R_{min} = 150 m and α = 2.15. Additional details on how the partly conflicting demands made on array performance were balanced by the adoption of this configuration can be found in Mykkeltveit (1985).

The NORESS array configuration is shown in Fig. 2. There is a center element denoted A0, 3 elements in the innermost ring (A-ring, nominal radius 150 m), 5 elements in the B-ring (radius 323 m), 7 elements in the C-ring (radius 693 m), and 9 elements in the D-ring (radius 1491 m, giving an array aperture of approximately 3 km). The short period stations at A0, C2, C4 and C7 are equipped with 3-component instruments. It is readily seen from Fig. 2 that there is a substantial range of intersensor separations present in the NORESS geometry, and that it offers a possibility of using widely different subgeometries for different signal frequencies.

Description of NORESS and ARCESS

The NORESS array was installed in southeastern Norway in the fall of 1984 (See Fig. 13 for location; array center coordinates are 60.735°N, 11.541°E) as a joint undertaking between NORSAR, the Defense Advanced Research Projects Agency and the Sandia National Laboratories. The array site is in a wooded area with relatively low population density. There is no human activity within the array except occasional forest work by the landowner. Competent bedrock with P wave velocities of the order of 5.5–6.0 km/s is found either at the surface, or underneath a layer of soil of thickness up to a few meters. The rock is of Precambrian age and is composed of gneisses and gabbro. A seismic reflection profile running north-south slightly east of the array center showed strong indications of a dipping reflector intersecting the surface in the southeastern part of the array (Mykkeltveit, 1987). Tomographic mapping of the velocity structure of the upper few kilometers beneath NORESS has been attempted by Ruud and Husebye (1990).

All NORESS short period instruments are placed in shallow vaults on concrete pads anchored to the bedrock. The seismometer housing is a fiberglass construction sealed to the concrete pad to prevent water leakage. The 3-component broad band seismometer at the array center is deployed in a 60 m deep borehole. All data from the vaults and borehole are transmitted to the hub building at the array center via trenched fiber optic cables, which are used since they are immune to electrical disturbances from, *e.g.*, nearby power lines and lightning. Each seismometer site is powered via buried cables from the hub building.

The NORESS short period instruments are of type GS-13, and the broad band borehole seismometer is a KS-36000 instrument. The conversion of data from analog to digital form takes place in the vaults and in the borehole. A 16 bits A/D converter is used, with 2 of the 16 bits used for gain ranging in steps of 1, 8, 32 and 128. Short period data are digitized at a rate of 40 Hz, whereas data from the broad band instrument are sampled both at 1 Hz for a long period band and at 10 Hz for an intermediate period band. The system transfer functions for the various passbands are shown in Fig. 3. The high frequency station that was integrated in NORESS in 1985 uses the analog output from the 3-component short period instrument at site A0, and digitizes this data at a rate of 125 Hz, using a 24 bits

A/D converter. A detailed description of this system is given by Ringdal *et al* (1990).

The ARCESS array installed in northern Norway in the fall of 1987 (array center coordinates are 69.534°N, 25.511°E; see location in Fig. 13) represented the first step towards a network of NORESS-type arrays. ARCESS is located at a distance of 1174 km from NORESS in an area of low population density and little or no industrial activity. The array sensors are deployed on gabbro, which is mostly exposed since the soil cover is nonexistent or very thin (up to 0.5 m). The short period seismometers are located in drums placed on the surface and covered with turf and moss, and the broad band instrument is in a 50 m deep borehole. Otherwise, the ARCESS field installation closely resembles that of NORESS: The geometries are nearly the same (deviations of the order of a few tens of meters in relative sensor positions exist due to adjustment to local terrain), and the seismic system with sensors and other electronic components are identical.

All data from the field installations of NORESS and ARCESS are collected by the hub processors at the central sites and transmitted in real time to the NORSAR data processing center at Kjeller. NORESS data are transmitted over a 64 Kbits/s land line, whereas a domestic satellite link with the same capacity is used to transmit ARCESS data. At Kjeller, the data are acquired on cyclic disk buffers that hold 72 hours of data for each array, processed, and permanently archived on magnetic tapes (on 8 mm video cassettes from February 1990). In this way, data from the last 3 days can be directly accessed from disk, whereas any data can be retrieved from the archive. NORESS and ARCESS data contain a substantial amount of environmental information (temperatures, humidities, wind speed and direction), as well as state-of-health and instrument calibration data, which are being analyzed automatically at Kjeller to assist in detecting system malfunction. The total amount of data generated by each array per day and stored in the archives is approximately 400 Mbytes.

Automatic Data Processing

With the amount of data received continuously from arrays like NORESS, it is of paramount importance that reliable schemes for fully automatic event detection and location in near real time be developed and implemented. The development of such algo-

rithms and procedures for NORESS went in parallel with the array design work in the early 1980s. The RONAPP (Regional ON-line Array Processing Package) code, described in Mykkeltveit and Bungum (1984) was the result of these efforts. In short, RONAPP detects phase arrivals using an STA/LTA-detector applied to a number of beams, estimates arrival azimuth and apparent velocity for the signals detected, and associates P- and S-arrivals for event location. Fig. 4 serves as an illustration of this procedure. It shows NORESS data for a presumed nuclear explosion in the White Sea region of the USSR on July 18, 1985, at a distance of 1550 km from NORESS. RONAPP detected Pn, Sn and Lg arrivals from this event, as indicated in the figure. The information on arrival azimuth and apparent velocity derived by computing frequency-wavenumber spectra for short data segments around the arrival times is used together with standard travel time tables to identify the phases and locate the event.

The RONAPP processing package has evolved through several generations into the version currently in use. The main underlying ideas, however, remain the same as those described in detail in Mykkeltveit and Bungum (1984). In the following description of the current version of the package we therefore focus on those aspects that have undergone changes since 1984 in light of experience gained.

Signal detection

The NORESS and ARCESS detection processing is similar to that of most other arrays: to enhance weak signals, a number of filtered beams (steered towards various hypothetical epicentral locations) are computed in real time and subjected to a conventional STA/LTA detector. Whenever the STA/LTA ratio exceeds a preset threshold, a detection is declared. When the threshold is exceeded for several beams within a 4 s long window, only one detection is declared and it is attributed to the beam with the highest STA/LTA ratio.

The real challenge in the design of the detector is the selection of a proper beam deployment with associated detection thresholds. Fig. 5 serves to illustrate some of the considerations involved. It shows NORESS data from a small event in western Norway, at an epicentral distance of approximately 350 km. The regional phases Pn, Pg, Sn and Lg are clearly seen after enhancement by filtering the data in widely different frequency bands and also displaying different components of the 3-axis station at site A0. It is found

for this particular event and many other events as well that the Pn and Pg phases are best observed on vertical channels, but in different frequency bands (here: 10–16 Hz for Pn and 3.5–5.5 Hz for Pg). The Lg phase stands out clearly in the 1–2 Hz band, also on vertical channels. The onset of the Sn phase, however, is very often found to have an impulsive character on the horizontal channels, and in a relatively high filter band (here: 5–8 Hz). This examples shows that a beam deployment designed for detection of regional phases must include several beams filtered within different narrow frequency bands, for each steering direction. It is also important to utilize the horizontal components of the 3-component stations for detection of phases like Sn.

The NORESS beam deployment in use since 13 April 1989 is given in Table 1. It is composed of 76 beams, out of which 66 are conventional, coherent ones. These 66 beams are aimed at detection of P-phases at all frequencies and are designed and deployed in accordance with the criterion that the gain loss due to missteering should be less than 3 dB for any signal from any direction, arriving at NORESS with an apparent velocity above 6.0 km/s. The subconfiguration defined for each of these beams is the one that has been found to provide the best SNR gain for the frequency band in question, see Kværna (1989). Incoherent beams are particularly suited for detection of secondary phases, which are often of an emergent nature. Ten such beams are included in the NORESS beam set, and are specifically aimed at detecting Sn (beams NH01–04) and Lg (beams NV01–06) arrivals. Details on incoherent beamforming are given in Ringdal *et al* (1975).

The determination of detection thresholds needs special attention, and one important aspect is the balancing of thresholds between the coherent and incoherent beams. The thresholds given in Table 1 were determined on the basis of operational experience as well as theoretical considerations on false alarm rates. Details of how this was done are given in Kværna *et al* (1987).

The beam set used at NORESS during 1 January 1985–13 April 1989 comprised 20 beams (see Ringdal, 1990), out of which 3 were incoherent, and with individual thresholds very similar to the ones of the new beam set. The 'old' beam deployment resulted in approximately 50,000 detections per year, and the new and more extensive beam set has caused an increase in the number of detections, mainly due to an improved beam coverage

for high frequencies. The ARCESS beam set is, since 1989, identical to that of NORESS, except for the steering parameters of the special beams directed towards Novaya Zemlya and Semipalatinsk. The number of detections on ARCESS exceeds that of NORESS; see Bratt *et al* (1990).

Estimation of signal attributes

Following the detection of a signal, best estimates of the arrival time, signal frequency and amplitude are obtained as outlined in Mykkeltveit and Bungum (1984). A frequency-wavenumber (f-k) spectrum is then computed for a 3 s long time window, starting 0.5 s before the detection time. Initially, the narrow-band f-k method described in Capon (1969) was used, but in 1989 a wide-band method described by Kværna and Doornbos (1986) was adopted. This analysis gives estimates of the arrival azimuth and apparent velocity of the detected signal. The signal is classified as P or S, corresponding to the apparent velocity being above or below 6.0 km/s, respectively. In addition, various attributes characterizing the particle motions are extracted from the 3-component stations, in accordance with a scheme devised by Jurkevics (1988). These attributes can be useful to distinguish Pn phases from Pg, and Sn phases from Lg, although consistent separation is difficult to achieve.

Phase association and event location

Simple rules and procedures are used to associate regional phases and determine event locations, based on the signal attributes estimated during the post-detection processing. These rules and procedures are given explicitly in Mykkeltveit and Bungum (1984). Modifications since then have essentially amounted to the following:

- Polarization information from the 3-component stations is used in an attempt to determine whether a P arrival is Pn or Pg, and whether an S-arrival is Sn or Lg.
- All regional signals with a phase assignment are used in the event location (previously, only Pn and Lg were used). Events are located using the TTAZLOC-algorithm by Bratt and Bache (1988).
- Phases are associated if their arrival azimuths deviate by less than 30° (previously

20°), and arrivals with apparent velocities exceeding 12 km/s are not considered regional and are not used in event location.

Experience from more than 5 years of continuous operation of NORESS (and more than 2 years with ARCESS) has shown that the procedure described in this chapter is successful in completely automatically detecting and locating with a reasonable accuracy a substantial number (typically 10–20 per day, depending on day-of-week) of small regional events. In particular, we want to emphasize that it has proved to be possible to design the detector, with its beam definitions, associated thresholds, etc., in such a way that detections are declared in the routine processing for almost all regional phases that can be caught by the human eye (including those that can only be seen on the beams), without causing a high number of irrelevant detections, *e.g.*, in the codas following the phase onsets. Too many detections will generally cause degradation of the performance of the phase association and event location steps. Fig. 6 serves to illustrate this point. It shows the final output from the automatic processing of NORESS data from a mining explosion in Estonia, at an epicentral distance of 795 km. The Pn, Sn and Lg phases have been detected and identified as such and subsequently used in the event location step. The Pn arrival was detected on the N073 beam with an STA/LTA ratio of 5.3. This beam is shown as trace no. 2 from the bottom of the plot. It has a steering azimuth of 90°, which is close to the azimuth of 96.5° estimated by the f-k analysis for this phase. The Sn phase was detected on beam NH02 (this beam is not shown), and the Lg phase on beam NV04, which is displayed in the form of a coherent beam as the bottom trace in Fig. 6. Two additional detections in the Lg coda (indicated by small arrows above the upper trace) show Lg type phase velocities and cause no difficulties in the automatic phase association and event location steps.

In addition to the regional arrivals, many teleseismic signals are detected by NORESS and ARCESS. In fact, the beam deployment in Table 1 was designed also with the teleseismic detection performance in mind, and several studies (*e.g.*, Ringdal, 1990) have testified to the excellent capabilities of NORESS and ARCESS in this regard. Fluctuations in the seismic noise field also give rise to many detections at both NORESS and ARCESS, and these are usually characterized by very low (Rayleigh type) apparent velocities. Kværna

(1990) has demonstrated that one class of such detections at NORESS can be correlated with the waterflow in a nearby major river.

Capabilities of NORESS and ARCESS

In this chapter, we will review and assess the individual capabilities of NORESS and ARCESS to detect and characterize regional signals, as well as their ability to locate regional events.

Signal detection capabilities

Numerous investigations have testified to the excellent capabilities of NORESS and ARCESS to suppress the noise and thus obtain considerable beamforming gain. NORESS noise suppression spectra taken hourly during a one-week period in July 1986 are shown in Fig. 7. A noise suppression spectrum is estimated as the ratio of the beam power spectrum to the average power spectrum, taken over all contributing sensors. For the specific subconfiguration (A0, C- and D-ring sensors) used in Fig. 7 the noise suppression is particularly effective in the 1.3–2.7 Hz band, where the suppression exceeds the $\sqrt{N}$ level expected for uncorrelated noise by up to 6 dB. The trend of the noise suppression curves in this frequency interval is the frequency-domain manifestation of the negative correlations observed in the curves in Fig. 1. Additional details on the NORESS noise suppression capabilities are found in Mykkeltveit *et al* (1990), where it is also demonstrated that these capabilities are stable over time, and furthermore show no strong dependency on the actual noise level. Noise level variations at NORESS have been extensively studied by Fyen (1990).

Taking also signal correlations into account, Kværna (1989) has conducted a study to determine the achievable P phase SNR gains at NORESS for various frequencies. He concludes that by carefully choosing the proper subgeometry at different frequencies, gains exceeding 10 dB can be consistently achieved over almost the entire band 0.5 to 10 Hz, with the highest average gains of 12–14 dB being obtained in the 1–4 Hz band.

The capability of NORESS and ARCESS to detect regional signals can be inferred from comparison with network bulletins for the region under study. Adopting the regional

bulletin published by the University of Helsinki as a reference, we have associated P-phases detected at ARCESS during January - March 1988 with events reported in this bulletin from the region of southern Finland and the surrounding areas of the western USSR, with epicentral distances relative to ARCESS in the range 800–1200 km. Fig. 8 gives a histogram of the number of reference events at each magnitude with the events detected by ARCESS marked specially. The figure further contains a detection probability curve with associated confidence limits, estimated by the maximum likelihood method of Ringdal (1975). We note that the 90 per cent P-wave detection capability in the region studied is close to $M_L = 2.5$. This can be compared to the NORESS threshold of $M_L = 2.7$ found by Ringdal (1986) for detection of P waves for events in the same region. If the criterion is relaxed to detection of *either* a P *or* an S arrival, the 90 per cent detection threshold is approximately 0.2 magnitude units lower.

The Novaya Zemlya test site is located at regional distance relative to both ARCESS and NORESS, and it is therefore of special interest to take a closer look at signals from this site. Fig. 9 shows data for an m_b 5.9 (NEIC) explosion on December 4, 1988, for both ARCESS and NORESS. For both arrays, raw (upper trace) and filtered data (lower trace) in the 5–10 Hz band are shown for the sensor at C1. The P wave was detected at ARCESS with an STA/LTA of 9136 (filter band 3–5 Hz for the detecting beam), and at NORESS with an STA/LTA of 796 (filter band 2.5–4.5 for the detecting beam). While the ARCESS detection capability is definitely better than that of NORESS for Novaya Zemlya, the difference is not as large as indicated by the STA/LTA values. Thus, the reason for the low value for NORESS is partly that the first P arrival has a low amplitude relative to the main phase that arrives about 4 seconds later. The maximum P amplitude is in fact similar for NORESS and ARCESS, even though the distance to NORESS is twice as large as the distance to ARCESS (20° and 10°, respectively). A comparison of the amplitudes of the data filtered in the 5–10 Hz band shows that the higher frequencies attenuate rapidly with distance. The secondary phase seen at ARCESS is Sn; the Lg phase is absent, most likely due to structural inhomogeneities and lateral variation of sediment thicknesses in the Barents Sea (Baumgardt, 1990). At NORESS, no secondary phases are readily visible in Fig. 9, but at closer examination a weak Sn phase is seen in a low frequency passband.

Comprehensive studies on spectral characteristics of regional phases in Fennoscandia have been carried out by several workers, see, *e.g.*, Suteau-Henson and Bache (1988) and Ringdal *et al* (1990).

Signal estimation capabilities

As mentioned in the previous chapter, a broad band f-k estimator (Kværna and Doornbos, 1986) has replaced the narrow band f-k analysis technique in the signal estimation stage of the online data processing of NORESS and ARCESS data. Before this was done, the performance of the two techniques was compared on several different data sets. One such set was a suite of 10 chemical explosions at a dam construction site (Blåsjø) in southern Norway at a distance of 301 km from NORESS. The two analysis techniques were applied to the Pn, Sn and Lg phases from the 10 events, and the results in terms of estimated arrival azimuth and apparent velocity are shown in Fig. 10. It is readily seen that the broad band method offers more stable results than the narrow band technique for all phases. The separation between the Sn and Lg phases is quite clear for this data set. It is difficult, however, in general to separate Sn and Lg based on apparent velocities alone.

Our experience with this broad band estimator is in general very good, and it appears to be the best tool currently available for estimation of arrival azimuth and apparent velocity from NORESS and ARCESS data. Occasionally though, it is observed for events with known epicenters that the estimates deviate substantially from the true values, and deviations as large as 10°–15° are observed for certain source regions even at high signal-to-noise ratios. These arrivals are coming in off azimuth due to structural inhomogeneities along the propagation path, and the estimates just reflect true propagation characteristics.

The 3-component stations at NORESS and ARCESS can also be used to infer slownesses. These are, however, less accurate than those obtained by the f-k analysis using the vertical sensors of the array, particularly at low values of SNR; see Harris (1990) and Henson (1990). In addition, 3-component estimates are susceptible to surface topography (Ødegaard *et al*, 1990). However, polarization information derived from 3-component stations can aid in the classification of the phases (Jepsen and Kennett, 1990).

Event location capabilities

In order to accurately locate regional events using one-array data, both the epicentral distance and event azimuth must be reliably determined.

The epicentral distance is determined on the basis of the travel time difference between the various regional phases. Our operational experience indicates that the key issue in this regard is the proper assignment of phase types (Sn, Lg, Rg) for the S waves detected. When only one S wave has been detected, it may be very difficult to decide whether it is an Sn or Lg arrival. An illustration of this is provided in Fig. 11, which shows the relative strength of Sn and Lg for six events recorded on a short period sensor of the NORSAR array (the NORSAR array is co-located with NORESS). Fig. 11 shows that Lg is strongly attenuated for certain propagation paths (as also observed in Fig. 9 for the Novaya Zemlya to ARCESS and NORESS paths), and that Sn likewise is sometimes not seen at all (event 1). It is well known that these differences are related to structural inhomogeneities along the propagation paths.

A misidentification of Sn as Lg (or vice-versa) will easily cause an error in the epicentral distance estimate of several hundred kilometers. However, when phase types are correctly assigned, the epicentral distance can usually be determined to within a few tens of kilometers. As a rule of thumb, an error of 1 s in the travel time difference between an S and a P phase results in an error of 6 km in the epicentral distance. The accuracy in the travel time difference largely depends on how well the arrival time of the S phase can be determined, and emergent arrivals represent a problem in this regard. When the phase onsets can be as reliably determined as shown in the example in Fig. 6, however, the travel time tables used become the limiting factor for accurate determination of epicentral distance.

Fig. 12 shows azimuth residuals for Pn phases detected at NORESS during 1985–1988. The data were derived as follows: The NORESS detection lists were searched for Pn phases that could be associated with regional events reported in the Helsinki bulletin for this 4-year period. The NORESS detection lists provide information on the arrival azimuth estimated for these Pn phases. The azimuth residuals (estimated azimuth minus 'true' azimuth) were computed and averaged on a grid of 1° x 2° blocks (north-south and east-west, respectively). These average values are then represented as shown in the

figure. For some of the blocks in the Estonian-Leningrad region of the USSR, averaging is done over several hundred azimuth residuals. Fig. 12 shows that the azimuth residuals are moderate (less than 2.5° in absolute value) for large geographical areas, but there are also areas with complicated behavior, like the Estonian-Leningrad region. We note that the arrival azimuths derived during 1985-88 were computed using the narrow band f-k method, and that the broad band method currently being used is likely to cause a reduction in the absolute values of the residuals. Anyway, the event locations will inevitably reflect such arrival azimuth uncertainties, and some kind of regional calibration will be needed, e.g., by taking information such as presented in Fig. 12 into account and correcting the arrival azimuths accordingly.

Network of NORESS-type Arrays

We have seen in the aforegoing chapter that single-array event locations may deviate from true locations by typically several tens of kilometers and even more, if phases are incorrectly assigned. The next step to improve the event location capability would be to install a network of NORESS-type arrays. This effort started with the installation of the ARCESS array in 1987, and continued with the deployment of the somewhat smaller FINESA array in Finland (Uski, 1990) in cooperation with the University of Helsinki, and the GERESS array in the Federal Republic of Germany (Harjes, 1990). Data from FINESA are since 1 January 1990 available in real time at the NORSAR data processing center at Kjeller and are being processed in the same way as data from ARCESS and NORESS. (The first version of the FINESA array was installed in 1985, but before 1 January 1990 data were recorded in trigger mode and on tapes at the array site only.) Data from GERESS will be available from the summer of 1990, and will also be transmitted to Kjeller for online processing.

In the following, we report on the findings of an investigation where data recorded at FINESA during experimental operation in March 1988 were used together with NORESS and ARCESS data in assessing the capabilities of this three-array network in locating events in the Fennoscandian region. A set of 10 event, for which there was at least one detected phase for each array, was selected for an event location experiment. The events

are listed in Table 2 and shown in Fig. 13. The event magnitudes range from less than 2.0 to 3.2. The epicentral locations for the 10 events are taken from the Helsinki bulletin.

The continuous processing of data recorded at each of the three regional arrays provides (among others) estimates of arrival times, arrival azimuths, and indication of phase type, as explained in the previous chapters. These parameters together with the associated uncertainties were used as input to the TTAZLOC program developed by Bratt and Bache (1988). TTAZLOC incorporates the arrival time and azimuth data into a generalized-inverse location estimation scheme, and can be applied to both single-array and multiple-array data. Table 2 gives the results of the location experiment. On the average, the joint three-array locations deviate from the network locations published in the Helsinki bulletin by 16 km. Two-array and one-array locations were computed for all combinations of events and array sub-networks, also using the TTAZLOC algorithm. The resulting average deviations from the network solutions are 26 and 68 km, respectively. Bratt and Bache (1988) and Bratt (1990) have also considered event mislocations using one-array and two-array data, and their results agree well with those reported here.

We see that the result for two-array locations represents a significant improvement over one-array locations, and that there is a further improvement when invoking data from three arrays. We consider the results reported here as quite promising, when taking the following into account:

- The arrival times used were those determined automatically by the online processing. It is conceivable that human intervention for adjustment of arrival times and/or refinement of the automatic procedure would improve the location estimates.
- Only standard travel time tables for the phases Pn, Sn and Lg were used. The introduction of regionalized travel time tables is likely to result in improvements.
- Master event location schemes of various kinds hold considerable promise and are expected to further enhance the capabilities of accurately locating regional events.

Discussion and Perspectives for the Future

This paper has summarized the main results from ten years of research at NORSAR

on regional arrays and their capabilities in detecting and characterizing seismic phases from events at regional distance. Assessments have also been given of the accuracy in determination of event locations from one-, two- and three-array data. In summary, we have found that P waves from events in the magnitude range 2.5–2.7 at distances around 1000 km are detected with a probability of 90 per cent, that the detector can be tuned so as to ensure detection also of emergent S wave arrivals, that the important signal attributes of regional phases (like arrival azimuth, apparent velocity, state of polarization, etc.) can be adequately characterized using a broad band f-k estimator on the vertical sensors of the array in combination with techniques for analysis of 3-component data, that the regional phases can be associated using a set of simple rules, and finally, that regional events can be located with an accuracy of the order of 15 km when data from a network of 3 arrays are used. It is noteworthy that these results are all obtained from fully automatic data processing, *i.e.*, without human intervention of any kind.

In several places in this paper, we have dealt with the issue of formulating rules that can be used in the automatic data processing. Such rules are generally suitable for the application of AI technologies in the form of so-called expert systems. While several such systems have been designed and experimentally applied to processing of regional array data (*e.g.*, Hiebert-Dodd, 1989; Mason *et al*, 1988), the most ambitious development so far is the Intelligent Monitoring System (IMS), described by Bache *et al* (1990). The aim of the IMS is to automate as much as possible the seismic data interpretation process, thus taking advantage of results such as those reported in this paper. It is currently being developed into a complete system for integrated, automatic processing of data from a network of regional arrays and single stations. The first version of the IMS has been operated at the Center for Seismic Studies in Arlington, Virginia, and at NORSAR since the fall of 1989. Initial results for the performance of IMS on data from NORESS and ARCESS are given by Bratt *et al* (1990).

The deployment of advanced regional arrays, and the associated development and implementation of automated and increasingly powerful data processing techniques represents one of the major advances in the field of seismic monitoring in recent years. Arrays of the NORESS/ARCESS design have demonstrated a capability to lower the detection

threshold by more than 0.5 magnitude units over a wide range of signal frequencies relative to traditional seismic stations. Furthermore, such regional arrays provide reliable phase identification and azimuth estimates which are particularly useful in locating weak events that are detected by only a few stations. In a seismic monitoring context, these are precisely those events that will need to be given the most emphasis.

Still, the process of exploiting the full potential of regional arrays is only at its beginning. Much research remains to be done in developing methods for integrated processing of data from a regional network composed of arrays and 3-component stations, and to assess its capabilities in a seismic monitoring context.

An essential aspect will be the further development of advanced processing technology to handle the data acquisition and quality control, data base organization, automatic interpretation and interactive computer graphics that will be required in an actual monitoring situation. From a seismological point of view, research topics to be addressed will include:

Signal processing: An important task will be to improve current methods for automatic detection, phase identification and onset time determination, with particular emphasis on Sn and Lg phases. Methods should be developed to exploit the potential for array processing of 3-component recordings offered by NORESS-type arrays, and to improve polarization analysis techniques at low SNR. There is a need to address the problem of how to automatically resolve multiple events, *i.e.*, two or more events with detected phases that are intermixed in time (*e.g.*, multiple mining explosions).

Regional calibration: An important aspect is the development of region-specific corrections for travel-time and azimuth anomalies. Furthermore, as attenuation characteristics of various seismic phase types (Pn, Pg, Sn, Lg, Rg) are highly path-dependent, it will be essential to accumulate region-specific knowledge in this regard. This will also contribute to the establishment of consistent regional magnitude scales, which should be developed and calibrated so as to be compatible with teleseismic magnitude.

Master event technique: The most powerful method currently available to obtain very precise epicenter and depth estimates is joint hypocentral determination using well-

recorded master events. This concept should be systematically extended to more general script-based pattern matching techniques, using the full array capabilities and incorporating both time domain and frequency domain features. This would be particularly useful to monitor specific mining locations and test sites, and should be accompanied by optimized beam and filter settings for such areas of special interest. The method for continuous threshold monitoring (Ringdal and Kværna, 1989) should be further developed and applied in such a context.

Source identification: Although efforts to develop regional discriminants so far have met with little success, this essential research should be pursued, aiming at obtaining systematic rules, developed on a region-specific basis. An important task will be to identify mining shots, and the very promising approach of characterizing spectral attributes of ripple-fired explosions should be given particular attention. The use of regional surface waves (*e.g.*, Rg) in source identification is also an important area of further research.

The key to further progress in this field would appear to be development and application of region-specific knowledge, both for the purpose of detection, location, depth estimation and source characterization. Much of the necessary knowledge can only be obtained through experimental operation over an extended period of time. The regional array network now being developed will in a unique way contribute to the establishment of such a knowledge base. The associated data management and processing facilities will ensure the availability of the data and the dissemination of the accumulated knowledge, and will thus aid in future efforts directed toward these research goals.

ACKNOWLEDGEMENTS

Over the years, numerous individuals both in Norway and elsewhere have contributed actively to the research reported on in this paper. In particular, the entire NORSAR staff is thanked for thcir efforts and enthusiasm, and we are especially indebted to Hilmar Bungum, Jan Fyen, Paul W. Larsen and Rune Paulsen for their valuable contributions to the regional array research program. This research was supported by the Advanced Research Projects Agency of the Department of Defense and was monitored by the Air Force Office of Scientific Research under Contract No. F49620-89-C-0038.

References

Bache, T.C., S.R. Bratt, J. Wang, R.M. Fung, C. Kobryn and J. Given (1990). The Intelligent Monitoring System, *Bull. Seism. Soc. Am.* (This volume).

Baumgardt, D.R. (1990). Investigation of teleseismic Lg blockage and scattering using regional arrays, *Bull. Seism. Soc. Am.* (This volume).

Bratt, S.R. and T.C. Bache (1988). Locating events with a sparse network of regional arrays, *Bull. Seism. Soc. Am.* **78**, 780–798.

Bratt, S.R., H.J. Swanger, R.J. Stead, F. Ryall, and T.C. Bache (1990). Initial results from the Intelligent Monitoring System, *Bull. Seism. Soc. Am.* (This volume).

Capon, J. (1969). High-resolution frequency-wavenumber spectrum analysis, *Proc. IEEE* **57**, 1408–1418.

Followill, F. and D.B. Harris (1983). Comments on small aperture array designs. Informal Report, Lawrence Livermore National Laboratory.

Fyen, J. (1990). Diurnal and seasonal variations in the microseismic noise level observed at the NORESS array, *Phys. Earth Planet. Int.*, in press.

Harjes, H.-P. (1990). Design and siting of a new regional array in Central Europe, *Bull. Seism. Soc. Am.* (This volume).

Harris, D.B. (1990). A comparison of the direction estimation performance of high-frequency seismic arrays and three-component stations, *Bull. Seism. Soc. Am.* (This volume).

Hiebert-Dodd, K.L. (1989). Assisting experts in their data analysis tasks — an AI approach, *Mathematics and Computers in Simulation* **31**, 475–484.

Henson, A. (1990). Estimating azimuth and slowness from three-component and array stations, *Bull. Seism. Soc. Am.* (This volume).

Jepsen, D.C. and B.L.N. Kennett (1990). Three component array analysis of regional seismograms, *Bull. Seism. Soc. Am.* (This volume).

Jurkevics, A. (1988). Polarization analysis of three-component array data, *Bull. Seism. Soc. Am.* 78, 1725–1743.

Kværna, T. (1989). On exploitation of small-aperture NORESS type arrays for enhanced P-wave detectability, *Bull. Seism. Soc. Am.* 79, 888–900.

Kværna, T. (1990). Sources of short-term fluctuations in the seismic noise level at NORESS, *Phys. Earth Planet. Int.*, in press.

Kværna, T. and D.J. Doornbos (1986). An integrated approach to slowness analysis with arrays and three-component stations, *Semiannual Tech. Summary, 1 October 1985 - 31 March 1986*, NORSAR Sci. Rep. No. 2-85/86, Kjeller, Norway.

Kværna, T., S. Kibsgaard and F. Ringdal (1987). False alarm statistics and threshold determination for regional event detection, *Semiannual Tech. Summary, 1 April - 30 September 1987*, NORSAR Sci. Rep. No. 1-87/88, Kjeller, Norway.

Mason, C.L., R.R. Johnson, R.M. Searfus, D. Lager and T. Canales (1988). A seismic event analyzer for nuclear test ban treaty verification. Technical Report UCRL-98069, Lawrence Livermore National Laboratory, Livermore, California.

Mykkeltveit, S. (1985). A new regional array in Norway: design work and results from analysis of data from a provisional installation, in *The VELA Program. A Twenty-Five Year Review of Basic Research*, A.U. Kerr, Editor, Defense Advanced Research Projects Agency.

Mykkeltveit, S. (1987). Local geology of the regional array sites in Norway, *Semiannual Tech. Summary, 1 April - 30 September 1987*, NORSAR Sci. Rep. No. 1-87/88, Kjeller, Norway.

Mykkeltveit, S., K. Åstebøl, D.J. Doornbos, and E.S. Husebye (1983). Seismic array configuration optimization, *Bull. Seism. Soc. Am.* 73, 173–186.

Mykkeltveit, S. and H. Bungum (1984). Processing of regional events using data from small-aperture arrays, *Bull. Seism. Soc. Am.* 74, 2313–2333.

Mykkeltveit, S., J. Fyen, F. Ringdal and T. Kværna (1990). Spatial characteristics of the NORESS noise field and implications for array detection processing, *Phys. Earth Planet. Int.*, in press.

Ødegaard, E., D.J. Doornbos, and T. Kværna (1990). Surface topographic effects at arrays and 3-component stations, *Bull. Seism. Soc. Am.* (This volume).

Ringdal, F. (1975). On the estimation of seismic detection thresholds, *Bull. Seism. Soc. Am.* **65**, 1631–1642.

Ringdal, F. (1986). Regional event detection using the NORESS array, *Semiannual Tech. Summary, 1 October 1985 – 31 March 1986*, NORSAR Sci. Rep. No. 2-85/86, Kjeller, Norway.

Ringdal, F. (1990). Teleseismic event detection using the NORESS array, with special reference to low-yield Semipalatinsk explosions, *Bull. Seism. Soc. Am.* (This volume).

Ringdal, F., E.S. Husebye, and A. Dahle (1975). P-wave envelope representation in event detection using array data, in *Exploitation of Seismograph Networks*, K.G. Beauchamp, Editor, Nordhoff-Leiden, The Netherlands, pp. 353–372.

Ringdal, F. and E.S. Husebye (1982). Application of arrays in the detection, location and identification of seismic events, *Bull. Seism. Soc. Am.* **72**, S201–S224.

Ringdal, F., S. Mykkeltveit, J. Fyen, and T. Kværna (1990). Spectral analysis of seismic signals and noise recorded at the NORESS high-frequency element. *Phys. Earth Planet. Int.*, in press.

Ringdal, F. and T. Kværna (1989). A multichannel processing approach to real time network detection, phase association, and threshold monitoring, *Bull. Seism. Soc. Am.* **79**, 1927–1940.

Ruud, B.O. and E.S. Husebye (1990). Exploring the upper crystalline crust: A joint interpretation of 3D imaging and reflection profiling at the NORESS array, *Tectonophysics*, in press.

Suteau-Henson, A. and T.C. Bache (1988). Spectral characteristics of regional phases recorded at NORESS, *Bull. Seism. Soc. Am.* 78, 708–725.

Uski, M. (1990). Event detection and location performance of the FINESA array in Finland, *Bull. Seism. Soc. Am.* (This volume).

TABLE CAPTIONS

Table 1. NORESS beam deployment. The table gives name of beam, steering velocity (in km/s), steering azimuth (in degrees), filter band (in Hz), STA/LTA threshold, and subconfiguration (in terms of which rings are included; the sensor at the central site A0 participates in *all* beams). The NH01–04 beams are incoherent and use the 8 horizontal channels (ne in the table, for north-south and east-west) of the stations at A0, C2, C4 and C7. The NV01–06 beams are also incoherent, and use vertical sensors as indicated. The remaining beams are conventional, coherent ones, using vertical channels only. The six coherent beams NH032–N037 are identical except for the steering azimuths, which have values of 30, 90, 150, 210, 270 and 330 degrees, respectively. The same pattern repeats for other coherent beams further down the table, and is indicated by an asterix in the azimuth column. Four special, coherent beams are steered towards each of the test sites at Semipalatinsk and Novaya Zemlya (at azimuths of 80 and 30 degrees, respectively).

Table 2. Results from TTAZLOC location experiments using data from NORESS, ARCESS and FINESA. Epicentral locations are given as reported in the Helsinki bulletin for a set of ten regional events that occurred between March 12 and March 18 of 1988. The table gives the deviation from these reference locations, as inferred from the TTAZLOC experiment described in the text.

Beam	Velocity	Azimuth	Filter band	Threshold	Conf.
N011	99999.9	0.0	0.5- 1.5	4.0	D
N021	99999.9	0.0	1.0- 3.0	4.0	CD
N031	99999.9	0.0	1.5- 3.5	4.0	CD
N032-037	11.0	*	1.5- 3.5	4.0	CD
N038	15.8	80.0	1.5- 3.5	3.5	CD
N039	10.0	30.0	1.5- 3.5	3.5	CD
N041	99999.9	0.0	2.0- 4.0	4.0	CD
N042-047	10.2	*	2.0- 4.0	4.0	CD
N048	15.8	80.0	2.0- 4.0	3.5	CD
N049	10.0	30.0	2.0- 4.0	3.5	CD
N051	99999.9	0.0	2.5- 4.5	4.0	BCD
N052-057	8.9	*	2.5- 4.5	4.0	BCD
N058	15.8	80.0	2.5- 4.5	3.5	BCD
N059	10.0	30.0	2.5- 4.5	3.5	BCD
N061	99999.9	0.0	3.0- 5.0	4.0	BCD
N062-067	10.5	*	3.0- 5.0	4.0	BCD
N068	15.8	80.0	3.0- 5.0	3.5	BCD
N069	10.0	30.0	3.0- 5.0	3.5	BCD
N071	99999.9	0.0	3.5- 5.5	4.0	BC
N072-077	11.1	*	3.5- 5.5	4.0	BC
N081	99999.9	0.0	4.0- 8.0	4.0	BC
N082-087	9.5	*	4.0- 8.0	4.0	BC
N091	99999.9	0.0	5.0-10.0	4.5	BC
N092-097	10.5	*	5.0-10.0	4.5	BC
N101	99999.9	0.0	8.0-16.0	4.5	AB
N102-107	9.9	*	8.0-16.0	4.5	AB
NH01	99999.9	0.0	2.0- 4.0	2.4	ne
NH02	99999.9	0.0	3.5- 5.5	2.4	ne
NH03	99999.9	0.0	5.0-10.0	2.4	ne
NH04	99999.9	0.0	8.0-16.0	2.5	ne
NV01	99999.9	0.0	0.5- 1.5	2.5	D
NV02	99999.9	0.0	1.0- 2.0	2.5	C
NV03	99999.9	0.0	1.5- 2.5	2.5	C
NV04	99999.9	0.0	2.0- 3.0	2.5	C
NV05	99999.9	0.0	2.0- 4.0	2.4	C
NV06	99999.9	0.0	3.5- 5.5	2.4	C

Table 1

Event No.	Network Lat.	Network Long.	Mag. M_L	No. of phases used	3-array 'error' (km)	Average 2-array 'error' (km)	Average 1-array 'error' (km)
1	67.1	20.6	<2	5	19	31	36
2	59.5	26.5	2.5	8	9	8	39
3	60.93	29.19	2.4	6	34	34	34
4	59.5	25.0	2.3	8	8	23	95
5	63.2	27.8	2.5	6	32	31	41
6	58.33	10.93	2.7	7	16	24	44
7	69.6	29.9	2.9	8	4	13	45
8	59.3	27.2	2.3	5	15	36	108
9	59.72	5.62	3.2	6	9	51	179
10	69.2	34.7	2.6	5	15	12	57
Average over 10 events					16	26	68

Table 2

FIGURE CAPTIONS

Fig. 1. NORESS noise correlations versus interstation separation for the two frequency bands 1–2 Hz and 3–4 Hz. The noise segment used is 30 s long and taken at 05:15 GMT on day 323 of 1985. Mean values and standard deviations within 100 m distance intervals are plotted on top of the population, except for short and long distances, where the number of correlation values is low.

Fig. 2. The geometry of the NORESS array. The instrument at the center is denoted A0. The other sensors are arranged in four concentric rings, the A-ring, B-ring, C-ring and D-ring. The type of instrumentation at each of the sensor sites is given in the legend.

Fig. 3. NORESS transfer functions (velocity sensitivity) for (from left to right) the long period, intermediate period, short period and high frequency band.

Fig. 4. The figure shows data from the vertical short period sensor at NORESS site A0 for an explosion in the White Sea region of the USSR on 18 July 1985. (ISC solution: origin time 21.14.57.7, epicenter at 65.96°, 40.86°E, depth 0 km and m_b 5.1). Also shown are broad band frequency-wavenumber spectra computed for the short data windows (indicated on top of the trace) centered around the onsets of the Pn, Sn and Lg arrivals.

Fig. 5. NORESS data for a small event in western Norway at epicentral distance 350 km. The various regional phases are enhanced by frequency filtering in different passbands, as explained in the text. A0Z denotes the vertical component of the short period sensor at the array center, whereas A0E is the horizontal east-west component at the same site.

Fig. 6. NORESS event processor plot for a mining explosion in Estonia. The plot shows data for the vertical channels of A0 and all instruments in the B- and C-rings. The two bottom traces are the beams on which the Pn (beam N073) and Lg phase (beam NV04) were detected. Note that the incoherent beam is plotted here as a coherent beam, but with the steering delays, filters and configuration as defined for the incoherent beam. Vertical bars across the panel indicate detected phases that are used in the TTAZLOC scheme (Bratt and Bache, 1988) to locate the event. Bulletin information is given in the upper

line on top of the traces. The second line contains information pertinent to the Pn phase.

Fig. 7. The figure shows 168 NORESS noise suppression spectra taken hourly during a one-week period in July 1986. The subgeometry used comprises the A0, C- and D-ring sensors. The horizontal line indicates the $\sqrt{N}$ (N = 17 in this case) suppression level.

Fig. 8. P-phase detection statistics for ARCESS for regional events in the distance range 800-1200 km, using the Helsinki bulletin as a reference. The upper part of the figure shows the distribution of events by magnitude with detected events corresponding to the hatched columns. The bottom part of the figure shows the estimated detection probability curve as a function of magnitude, with the observed detection percentages marked as asterisks. The stippled curves mark the 90 per cent confidence limits.

Fig. 9. NORESS and ARCESS data for the sensor at C1 for a nuclear test at Novaya Zemlya on December 4, 1988. Data are shown both unfiltered (upper trace) and filtered in the band 5–10 Hz (lower trace) for both arrays.

Fig. 10. The figure shows the results of the narrow band (left) and broad band (right) f-k estimator applied to the Pn, Sn and Lg phases observed at NORESS from a suite of 10 chemical explosions at a dam construction site in southern Norway. The processing frequencies for the narrow band method were 7 Hz for Pn and 4 Hz for Sn and Lg. For the broad band method estimates are given for the frequency intervals 5.25–8.75 Hz for Pn and 3–5 Hz for Sn and Lg.

Fig. 11. Illustration of variation of relative importance of the phases Sn and Lg for six events with locations as indicated in the map. The standard group velocities of 4.5 and 3.5 km/s, commonly assigned to Sn and Lg, respectively, are marked by dashed lines. The upper three traces cover the distance interval 480–550 km, while the lower three traces correspond to epicentral distances in the range 1225–1320 km. The location of the NORSAR array is denoted by a ring on the map, and the traces are from NORSAR seismometer 02B01. The data are bandpass filtered 1–5 Hz. The reduction velocity is 8.0 km/s.

Fig. 12. Azimuth residuals (AR = estimated azimuth minus 'true' azimuth, in degrees) for Pn phases detected at NORESS during 1985-88, for events reported in the Helsinki bulletin. See the text for further explanation.

Fig. 13. The map shows the location of the three regional arrays NORESS and ARCESS in Norway and FINESA in Finland, as well as the location of the ten events used in the TTAZLOC location estimation experiment.

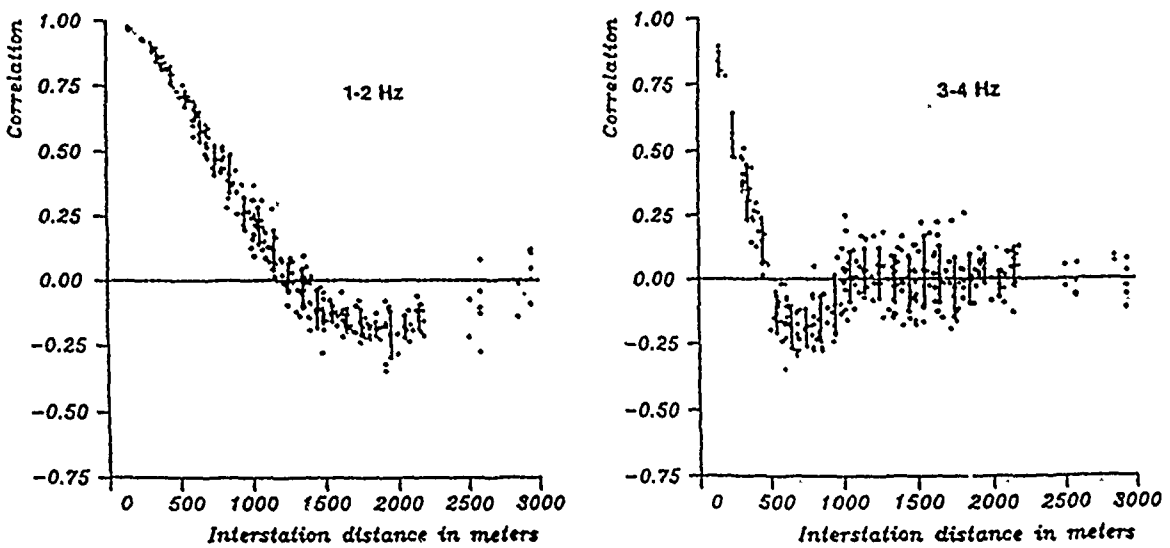
1-2 Hz
3-4 Hz
Correlation
1.00
0.75
0.50
0.25
0.00
-0.25
-0.50
-0.75
0
500
1000
1500
2000
2500
3000
Interstation distance in meters

Fig. 1

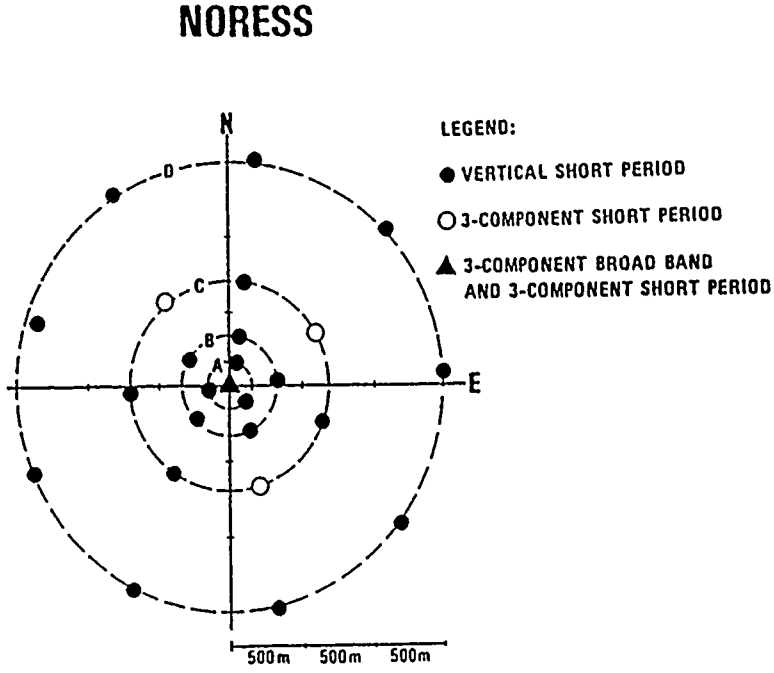
NORESS
N
E
D
C
B
A
LEGEND:
VERTICAL SHORT PERIOD
3-COMPONENT SHORT PERIOD
3-COMPONENT BROAD BAND
AND 3-COMPONENT SHORT PERIOD
500m
500m
500m

Fig. 2

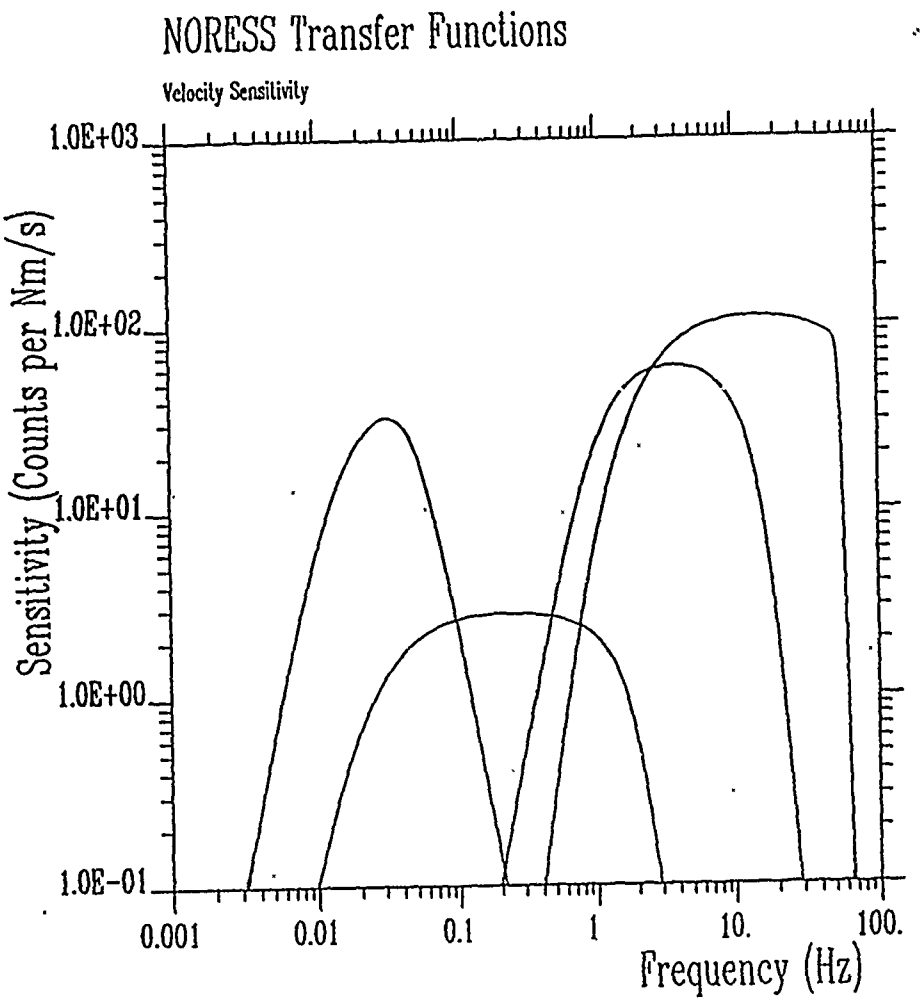
NORESS Transfer Functions
Velocity Sensitivity
1.0E+03
1.0E+02
1.0E+01
1.0E+00
1.0E-01
Sensitivity (Counts per Nm/s)
0.001
0.01
0.1
1
10.
100.
Frequency (Hz)

Fig. 3

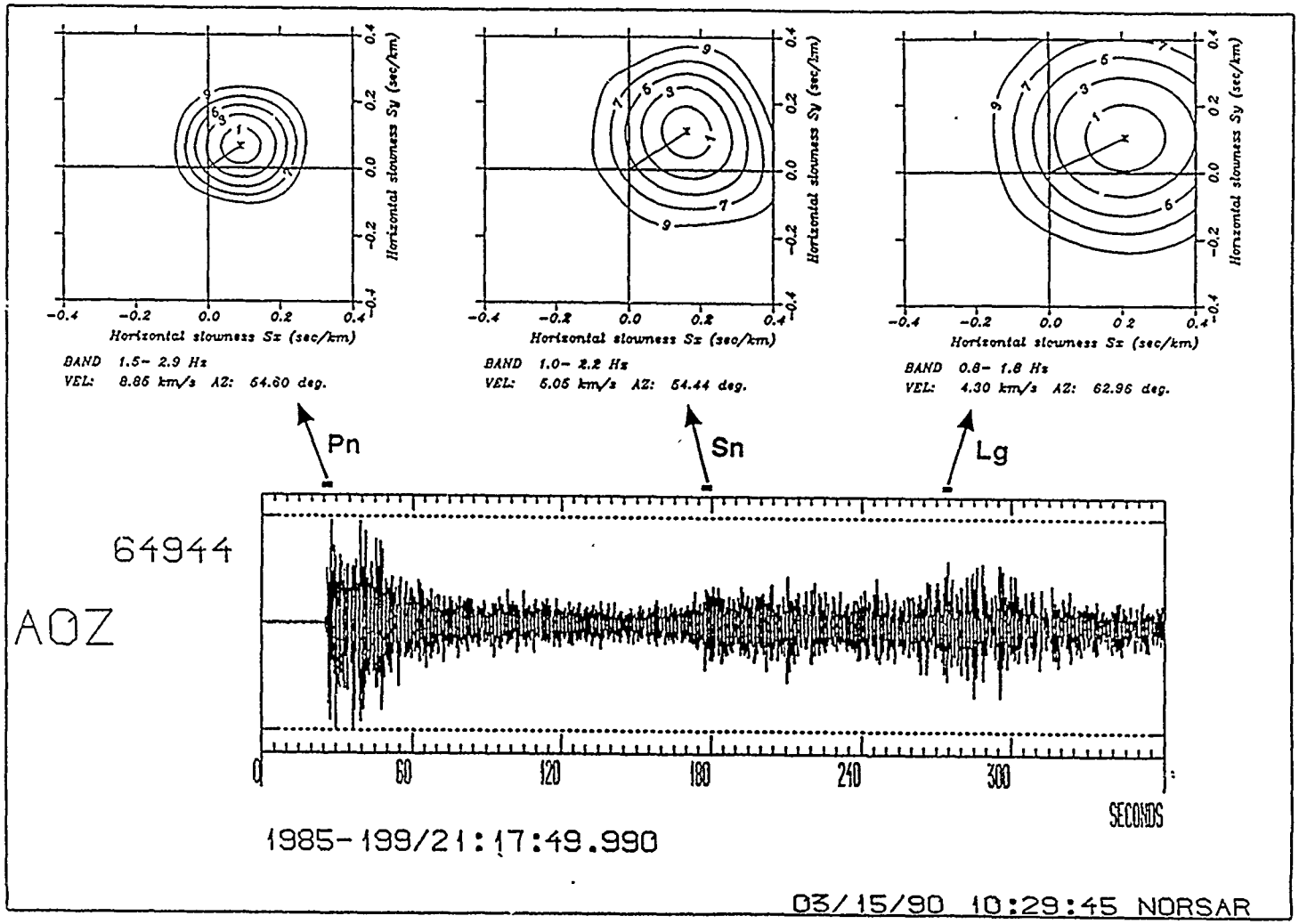
Horizontal slowness Sx (sec/km)
Horizontal slowness Sy (sec/km)
BAND 1.5- 2.9 Hz
VEL: 8.86 km/s AZ: 64.80 deg.
BAND 1.0- 2.2 Hz
VEL: 5.05 km/s AZ: 54.44 deg.
BAND 0.8- 1.8 Hz
VEL: 4.30 km/s AZ: 62.96 deg.
Pn
Sn
Lg
64944
AOZ
0
60
120
180
240
300
SECONDS
1985-199/21:17:49.990
03/15/90 10:29:45 NORSAR

Fig. 4

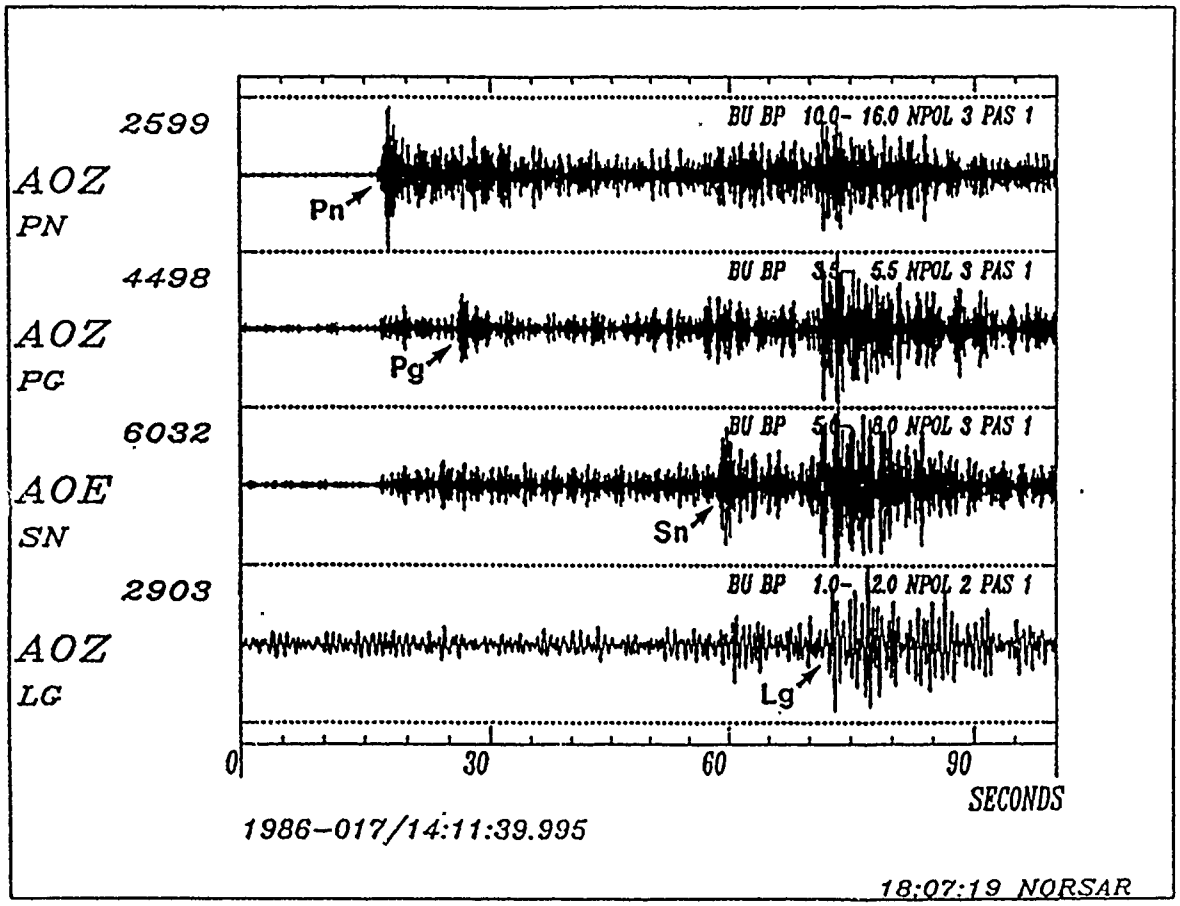
2599
AOZ
PN
BU BP 10.0- 16.0 NPOL 3 PAS 1
Pn
4498
AOZ
PG
BU BP 3.5- 5.5 NPOL 3 PAS 1
Pg
6032
AOE
SN
BU BP 5.0- 8.0 NPOL 3 PAS 1
Sn
2903
AOZ
LG
BU BP 1.0- 2.0 NPOL 2 PAS 1
Lg
0
30
60
90
SECONDS
1986-017/14:11:39.995
18:07:19 NORSAR

Fig. 5

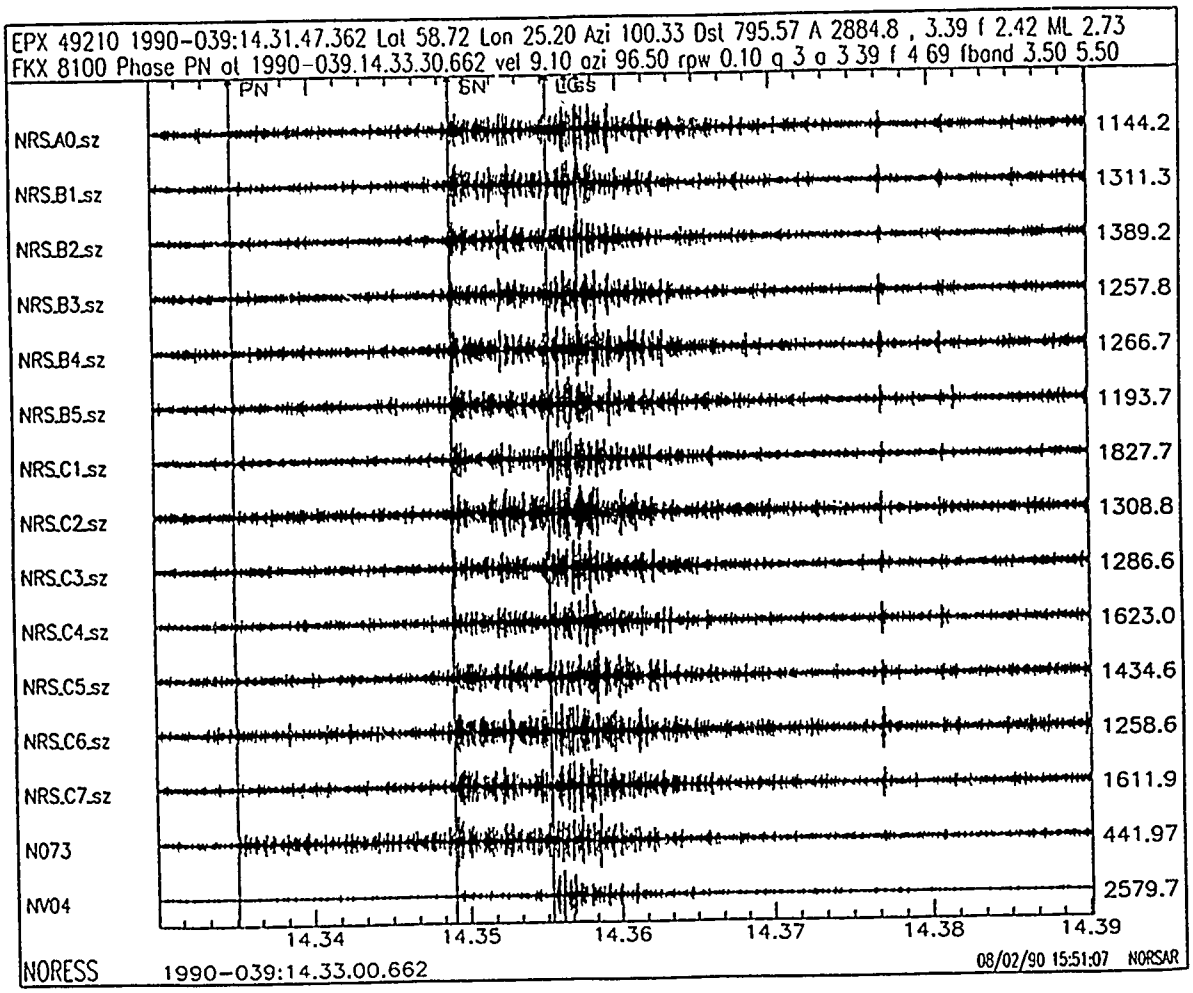
EPX 49210 1990-039:14.31.47.362 Lat 58.72 Lon 25.20 Azi 100.33 Dst 795.57 A 2884.8 , 3.39 f 2.42 ML 2.73
FKX 8100 Phase PN at 1990-039.14.33.30.662 vel 9.10 azi 96.50 rpw 0.10 q 3 a 3.39 f 4 69 fband 3.50 5.50
PN
SN
LG
NRS.A0.sz
NRS.B1.sz
NRS.B2.sz
NRS.B3.sz
NRS.B4.sz
NRS.B5.sz
NRS.C1.sz
NRS.C2.sz
NRS.C3.sz
NRS.C4.sz
NRS.C5.sz
NRS.C6.sz
NRS.C7.sz
N073
NV04
1144.2
1311.3
1389.2
1257.8
1266.7
1193.7
1827.7
1308.8
1286.6
1623.0
1434.6
1258.6
1611.9
441.97
2579.7
14.34
14.35
14.36
14.37
14.38
14.39
NORESS
1990-039:14.33.00.662
08/02/90 15:51:07 NORSAR

Fig. 6

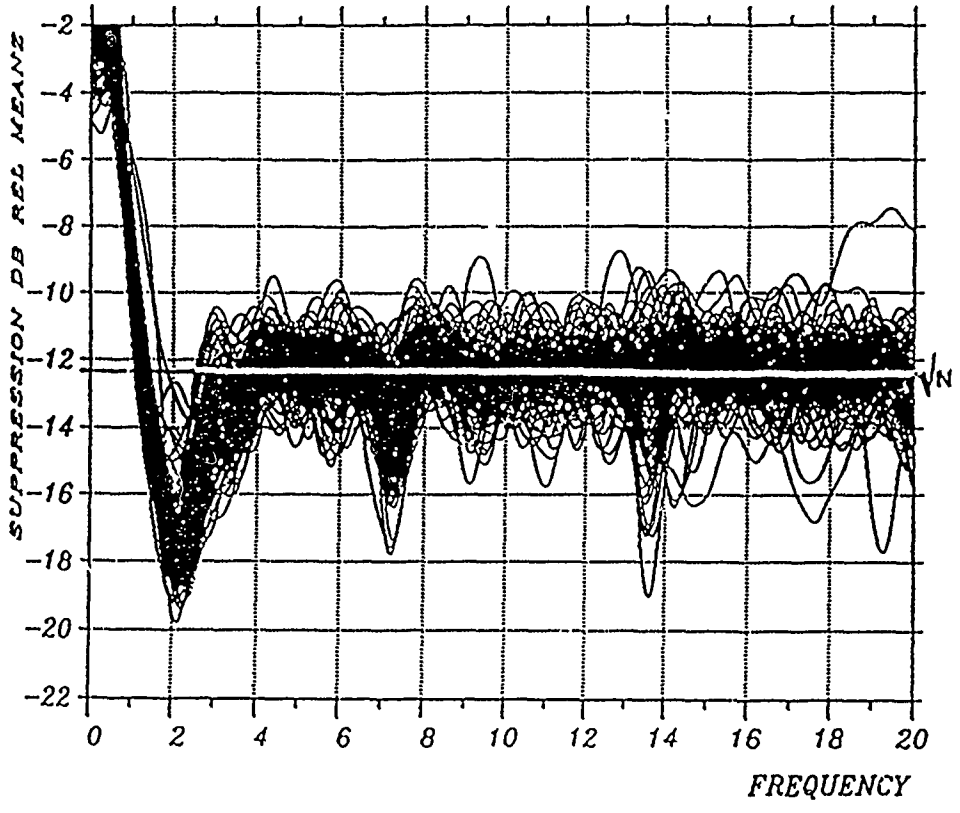
SUPPRESSION DB REL MEANZ
-2
-4
-6
-8
-10
-12
-14
-16
-18
-20
-22
0
2
4
6
8
10
12
14
16
18
20
FREQUENCY
√N

Fig. 7

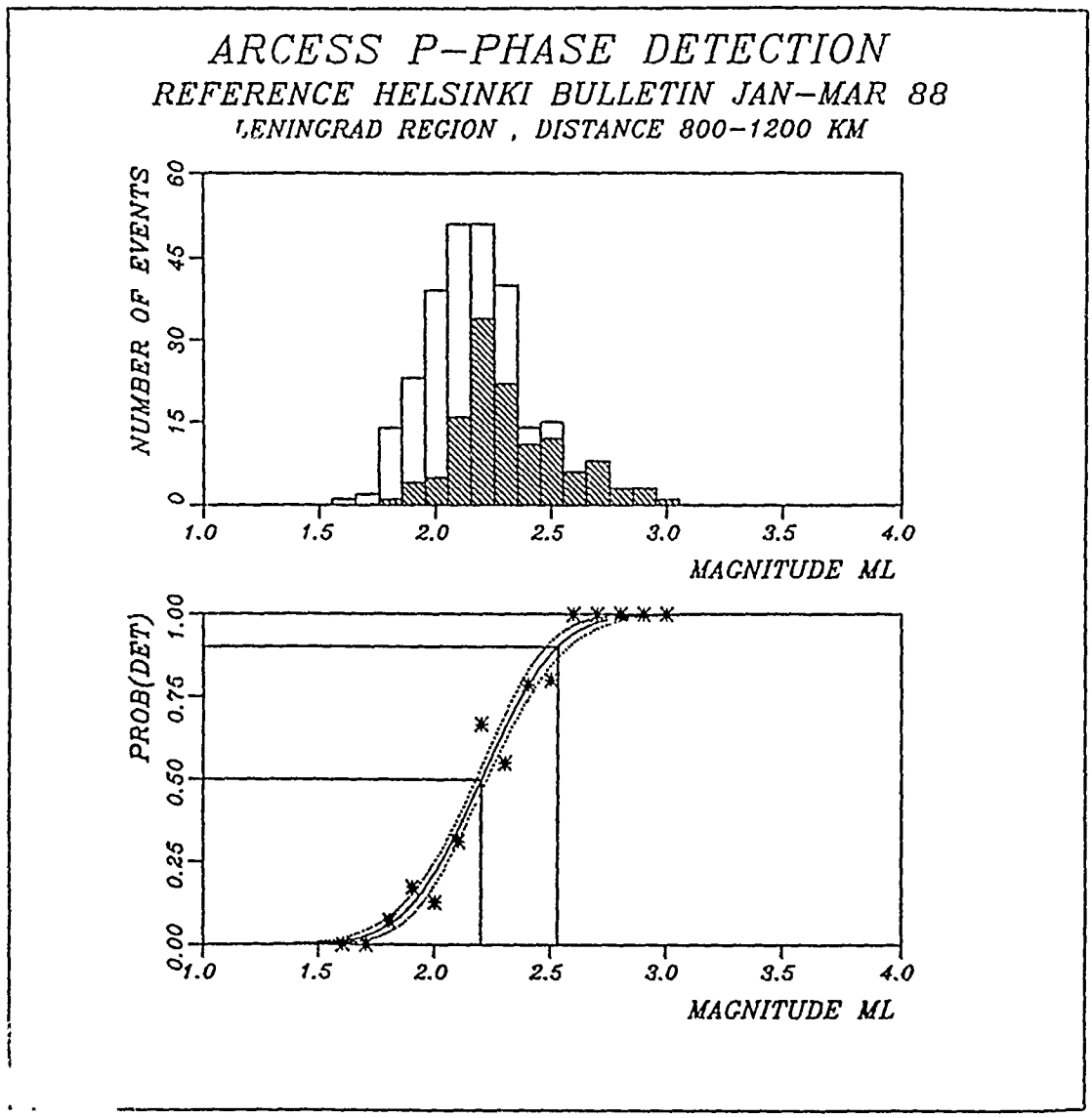
ARCESS P-PHASE DETECTION
REFERENCE HELSINKI BULLETIN JAN-MAR 88
LENINGRAD REGION , DISTANCE 800-1200 KM
NUMBER OF EVENTS
0
15
30
45
60
1.0
1.5
2.0
2.5
3.0
3.5
4.0
MAGNITUDE ML
PROB(DET)
0.00
0.25
0.50
0.75
1.00
1.0
1.5
2.0
2.5
3.0
3.5
4.0
MAGNITUDE ML

Fig. 8

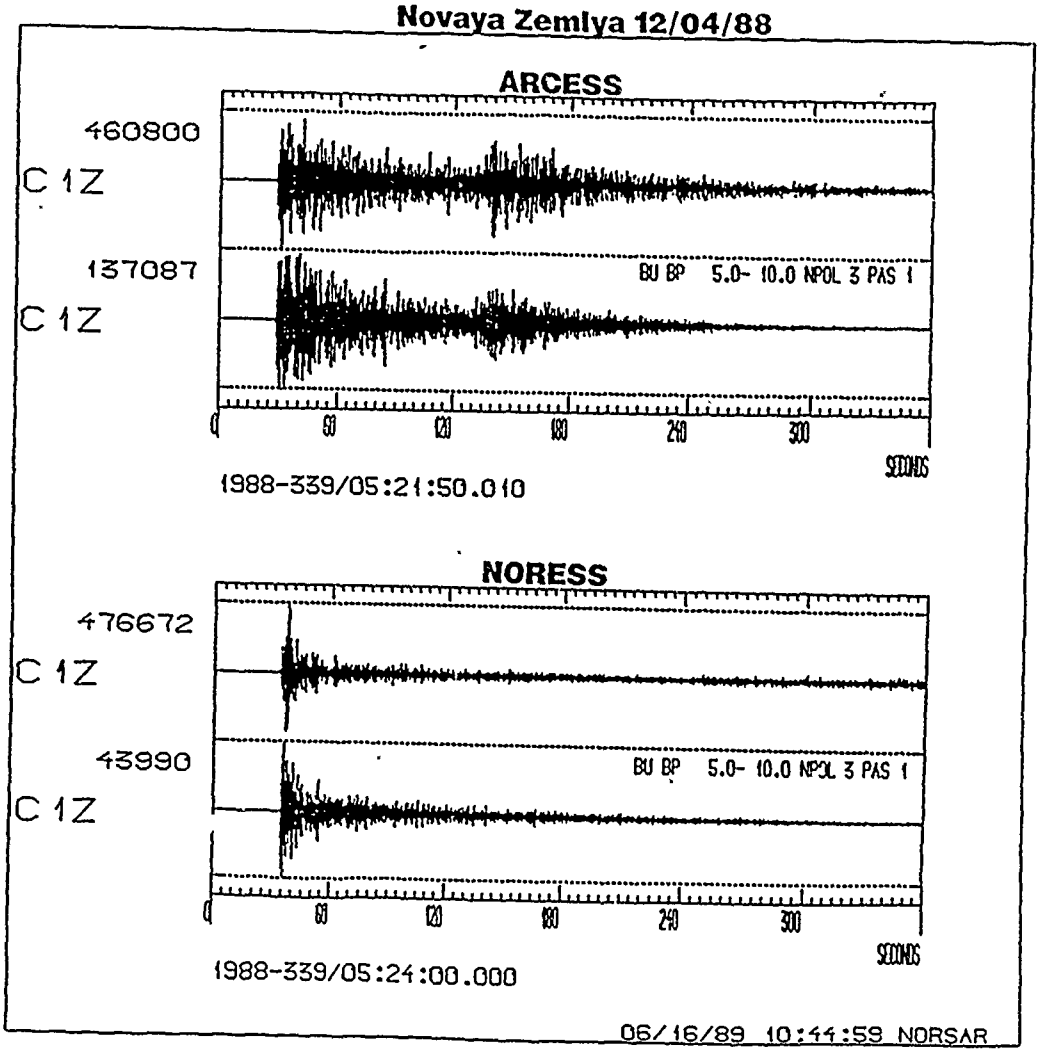
Novaya Zemlya 12/04/88
ARCESS
460800
C 1Z
137087
C 1Z
BU BP 5.0- 10.0 NPOL 3 PAS 1
0
60
120
180
240
300
SECONDS
1988-339/05:21:50.010
NORESS
476672
C 1Z
43990
C 1Z
BU BP 5.0- 10.0 NPOL 3 PAS 1
0
60
120
180
240
300
SECONDS
1988-339/05:24:00.000
06/16/89 10:44:59 NORSAR

Fig. 9

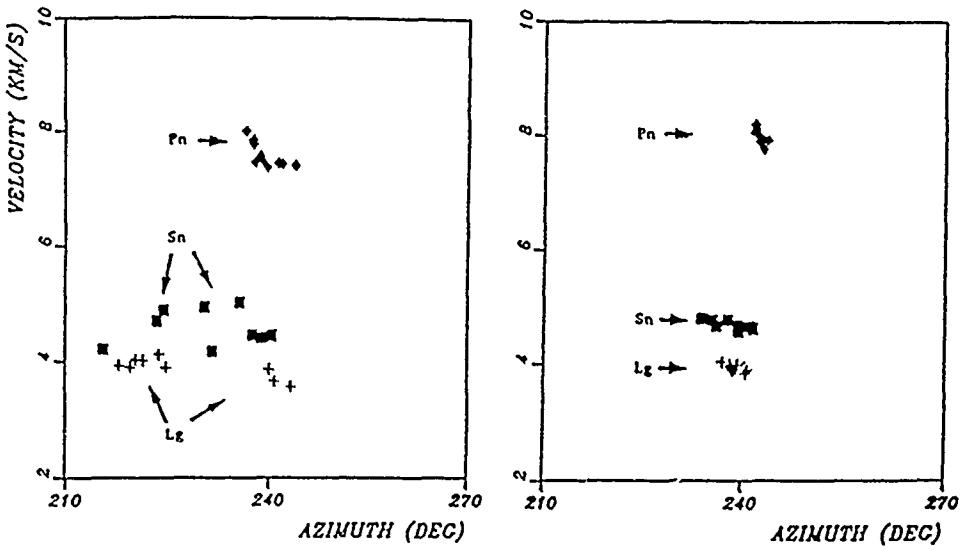
VELOCITY (KM/S)
10
8
6
4
2
Pn
Sn
Lg
210
240
270
AZIMUTH (DEC)
10
8
6
4
2
Pn
Sn
Lg
210
240
270
AZIMUTH (DEC)

Fig. 10

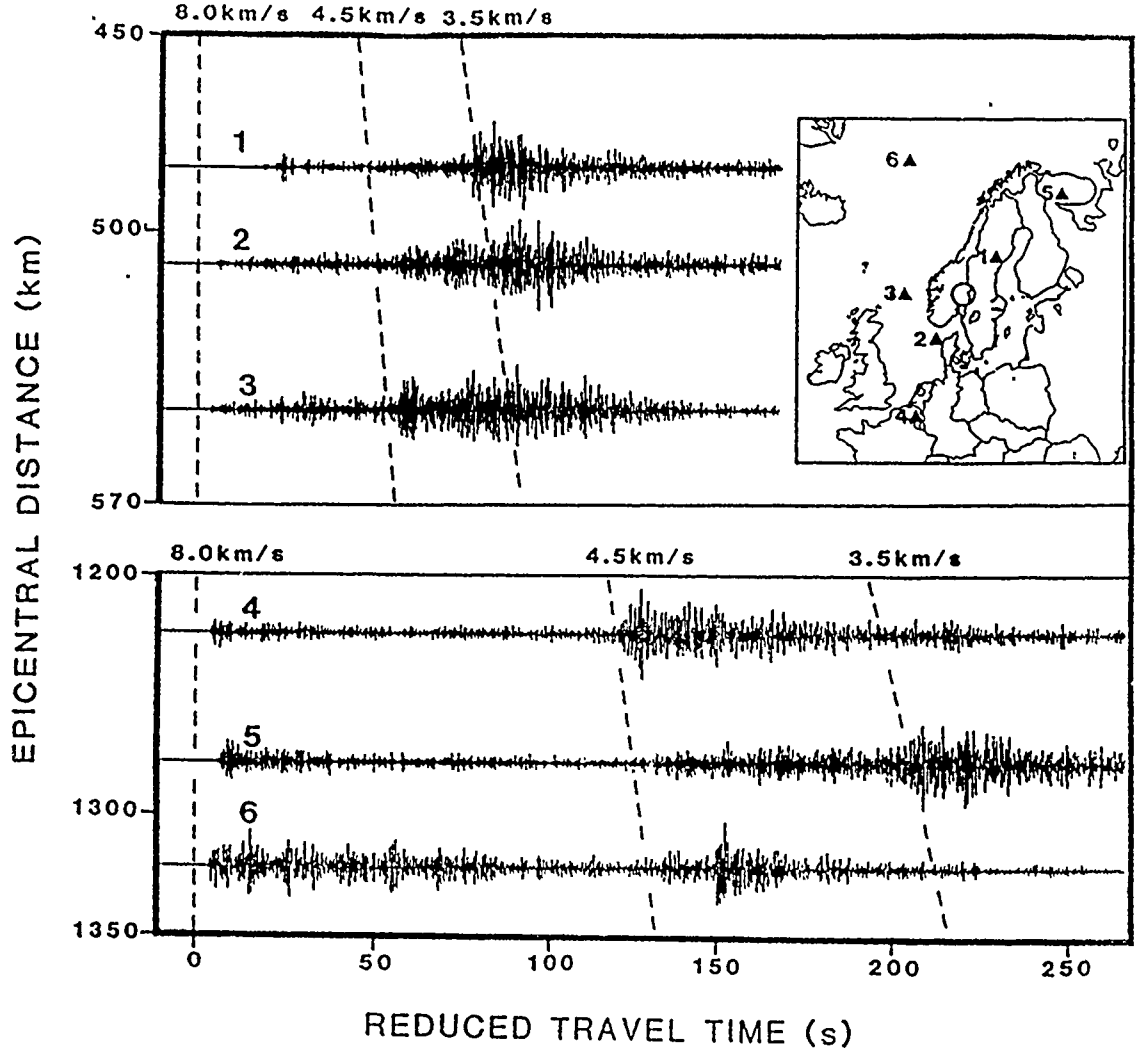
8.0km/s 4.5km/s 3.5km/s
450
500
570
1
2
3
6▲
5▲
1▲
3▲
2▲
4▲
8.0km/s
4.5km/s
3.5km/s
1200
1300
1350
4
5
6
0
50
100
150
200
250
EPICENTRAL DISTANCE (km)
REDUCED TRAVEL TIME (s)

Fig. 11

Negative azimuth residuals

Azimuths within 2.5 degrees of 'true' values

Positive azimuth residuals

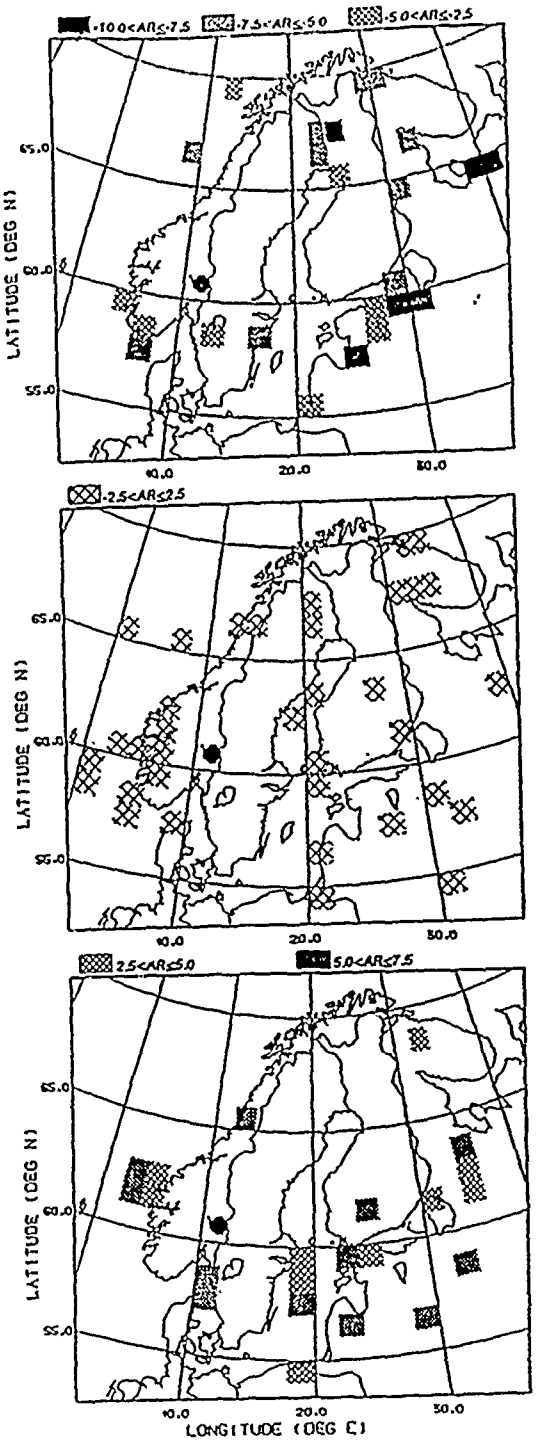

Fig. 12

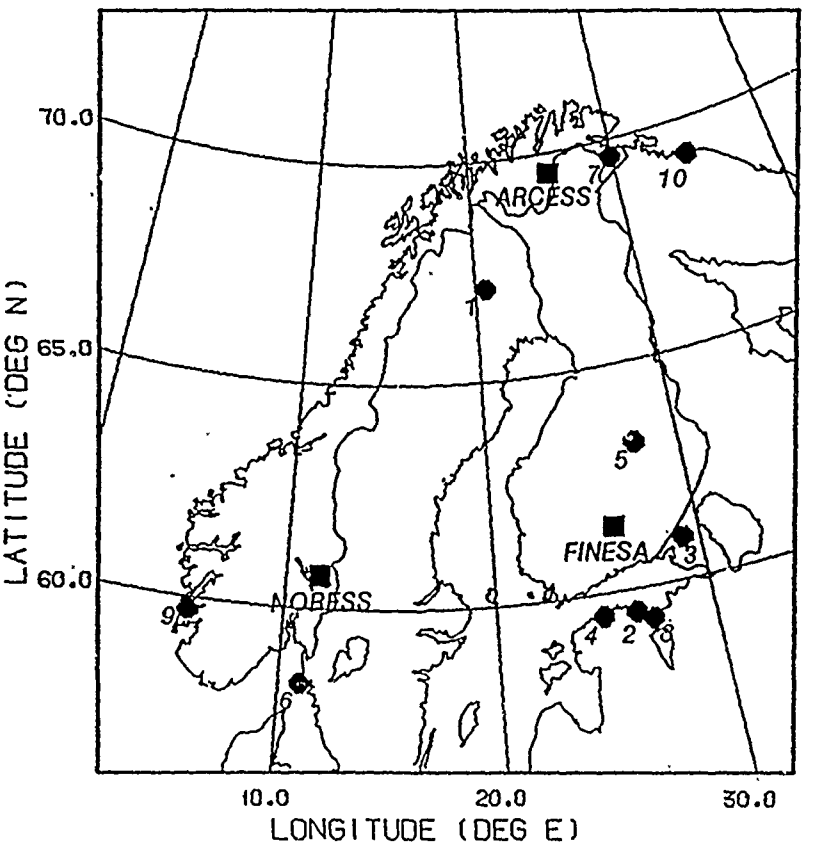
70.0
65.0
60.0
LATITUDE (DEG N)
10.0
20.0
30.0
LONGITUDE (DEG E)
ARCESS
FINESA
NORESS
1
2
3
4
5
6
7
8
9
10

Fig. 13

CONTRACTORS (UNITED STATES)

Prof. Thomas Ahrens
Seismological Lab, 252-21
Division of Geological & Planetary Sciences
California Institute of Technology
Pasadena, CA 91125

Prof. Charles B. Archambeau
CIRES
University of Colorado
Boulder, CO 80309

Dr. Thomas C. Bache, Jr.
Science Applications Int'l Corp.
10260 Campus Point Drive
San Diego, CA 92121 (2 copies)

Prof. Muawia Barazangi
Institute for the Study of the Continent
Cornell University
Ithaca, NY 14853

Dr. Douglas R. Baumgardt
ENSCO, Inc
5400 Port Royal Road
Springfield, VA 22151-2388

Prof. Jonathan Berger
IGPP, A-025
Scripps Institution of Oceanography
University of California, San Diego
La Jolla, CA 92093

Dr. Lawrence J. Burdick
Woodward-Clyde Consultants
566 El Dorado Street
Pasadena, CA 91109-3245

Dr. Jerry Carter
Center for Seismic Studies
1300 North 17th St., Suite 1450
Arlington, VA 22209-2308

Dr. Karl Coyner
New England Research, Inc.
76 Olcott Drive
White River Junction, VT 05001

Prof. Vernon F. Cormier
Department of Geology & Geophysics
U-45, Room 207
The University of Connecticut
Storrs, CT 06268

Professor Anton W. Dainty
Earth Resources Laboratory
Massachusetts Institute of Technology
42 Carleton Street
Cambridge, MA 02142

Prof. Steven Day
Department of Geological Sciences
San Diego State University
San Diego, CA 92182

Dr. Zoltan A. Der
ENSCO, Inc.
5400 Port Royal Road
Springfield, VA 22151-2388

Prof. John Ferguson
Center for Lithospheric Studies
The University of Texas at Dallas
P.O. Box 830688
Richardson, TX 75083-0688

Dr. Mark D. Fisk
Mission Research Corporation
735 State Street
P. O. Drawer 719
Santa Barbara, CA 93102

Prof. Stanley Flatte
Applied Sciences Building
University of California
Santa Cruz, CA 95064

Dr. Alexander Florence
SRI International
333 Ravenswood Avenue
Menlo Park, CA 94025-3493

Prof. Stephen Grand
University of Texas at Austin
Department of Geological Sciences
Austin, TX 78713-7909

Prof. Henry L. Gray
Vice Provost and Dean
Department of Statistical Sciences
Southern Methodist University
Dallas, TX 75275

Dr. Indra Gupta
Teledyne Geotech
314 Montgomery Street
Alexandria, VA 22314

Prof. David G. Harkrider
Seismological Laboratory
Division of Geological & Planetary Sciences
California Institute of Technology
Pasadena, CA 91125

Prof. Donald V. Helmberger
Seismological Laboratory
Division of Geological & Planetary Sciences
California Institute of Technology
Pasadena, CA 91125

Prof. Eugene Herrin
Institute for the Study of Earth and Man
GeophysicalLaboratory
Southern Methodist University
Dallas, TX 75275

Prof . Robert B. Herrmann
Department of Earth & Atmospheric Sciences
St. Louis University
St. Louis, MO 63156

Prof. Bryan Isacks
Cornell University
Department of Geological Sciences
SNEE Hall
Ithaca, NY 14850

Dr. Rong-Song Jih
Teledyne Geotech
314 Montgomery Street
Alexandria, VA 22314

Prof. Lane R. Johnson
Seismographic Station
University of California
Berkeley, CA 94720

Prof. Alan Kafka
Department of Geology & Geophysics
Boston College
Chestnut Hill, MA 02167

Dr. Richard LaCoss
MIT-Lincoln Laboratory
M-200B
P. O. Box 73
Lexington, MA 02173-0073 (3 copies)

Prof Fred K. Lamb
University of Illinois at Urbana-Champaign
Department of Physics
1110 West Green Street
Urbana, IL 61801

Prof. Charles A. Langston
Geosciences Department
403 Deike Building
The Pennsylvania State University
University Park, PA 16802

Prof. Thorne Lay
Institute of Tectonics
Earth Science Board
University of California, Santa Cruz
Santa Cruz, CA 95064

Prof. Arthur Lerner-Lam
Lamont-Doherty Geological Observatory
of Columbia University
Palisades, NY 10964

Dr. Christopher Lynnes
Teledyne Geotech
314 Montgomery Street
Alexandria, VA 22314

Prof. Peter Malin
University of California at Santa Barbara
Institute for Crustal Studies
Santa Barbara, CA 93106

Dr. Randolph Martin, III
New England Research, Inc.
76 Olcott Drive
White River Junction, VT 05001

Prof. Thomas V. McEvilly
Seismographic Station
University of California
Berkeley, CA 94720

Dr. Keith L. McLaughlin
S-CUBED
A Division of Maxwell Laboratory
P.O. Box 1620
La Jolla, CA 92038-1620

Prof. William Menke
Lamont-Doherty Geological Observatory
of Columbia University
Palisades, NY 10964

Stephen Miller
SRI International
333 Ravenswood Avenue
Box AF 116
Menlo Park, CA 94025-3493

Prof. Bernard Minster
IGPP, A-025
Scripps Institute of Oceanography
University of California, San Diego
La Jolla, CA 92093

Prof. Brian J. Mitchell
Department of Earth & Atmospheric Sciences
St. Louis University
St. Louis, MO 63156

Mr. Jack Murphy
S-CUBED, A Division of Maxwell Laboratory
11800 Sunrise Valley Drive
Suite 1212
Reston, VA 22091 (2 copies)

Dr. Bao Nguyen
GL/LWH
Hanscom AFB, MA 01731-5000

Prof. John A. Orcutt
IGPP, A-025
Scripps Institute of Oceanography
University of California, San Diego
La Jolla, CA 92093

Prof. Keith Priestley
University of Cambridge
Bullard Labs, Dept. of Earth Sciences
Madingley Rise, Madingley Rd.
Cambridge CB3 OEZ, ENGLAND

Prof. Paul G. Richards
Lamont Doherty Geological Observatory
of Columbia University
Palisades, NY 10964

Dr. Wilmer Rivers
Teledyne Geotech
314 Montgomery Street
Alexandria, VA 22314

Prof. Charles G. Sammis
Center for Earth Sciences
University of Southern California
University Park
Los Angeles, CA 90089-0741

Prof. Christopher H. Scholz
Lamont-Doherty Geological Observatory
of Columbia University
Palisades, NY 10964

Thomas J. Sereno, Jr.
Science Application Int'l Corp.
10260 Campus Point Drive
San Diego, CA 92121

Prof. David G. Simpson
Lamont-Doherty Geological Observatory
of Columbia University
Palisades, NY 10964

Dr. Jeffrey Stevens
S-CUBED
A Division of Maxwell Laboratory
P.O. Box 1620
La Jolla, CA 92038-1620

Prof. Brian Stump
Institute for the Study of Earth & Man
Geophysical Laboratory
Southern Methodist University
Dallas, TX 75275

Prof. Jeremiah Sullivan
University of Illinois at Urbana-Champaign
Department of Physics
1110 West Green Street
Urbana, IL 61801

Prof. Clifford Thurber
University of Wisconsin-Madison
Department of Geology & Geophysics
1215 West Dayton Street
Madison, WS 53706

Prof. M. Nafi Toksoz
Earth Resources Lab
Massachusetts Institute of Technology
42 Carleton Street
Cambridge, MA 02142

Prof. John E. Vidale
University of California at Santa Cruz
Seismological Laboratory
Santa Cruz, CA 95064

Prof. Terry C. Wallace
Department of Geosciences
Building #77
University of Arizona
Tucson, AZ 85721

Dr. Raymond Willeman
GL/LWH
Hanscom AFB, MA 01731-5000

Dr. Lorraine Wolf
GL/LWH
Hanscom AFB, MA 01731-5000

Dr. William Wortman
8560 Cinderbed Road
Suite # 700
Newington, VA 22122

Dr. Monem Abdel-Gawad
Rockwell International Science Center
1049 Camino Dos Rios
Thousand Oaks, CA 91360

Prof. Keiiti Aki
Center for Earth Sciences
University of Southern California
University Park
Los Angeles, CA 90089-0741

Prof. Shelton S. Alexander
Geosciences Department
403 Deike Building
The Pennsylvania State University
University Park, PA 16802

Dr. Kenneth Anderson
BBNSTC
Mail Stop 14/1B
Cambridge, MA 02238

Dr. Ralph Archuleta
Department of Geological Sciences
University of California at Santa Barbara
Santa Barbara, CA 93102

Dr. Jeff Barker
Department of Geological Sciences
State University of New York
at Binghamton
Vestal, NY 13901

Dr. Susan Beck
Department of Geosciences, .Bldg # 77
University of Arizona
Tucson, AZ 85721

Dr. T.J. Bennett
S-CUBED
A Division of Maxwell Laboratory
11800 Sunrise Valley Drive, Suite 1212
Reston, VA 22091

Mr. William J. Best
907 Westwood Drive
Vienna, VA 22180

Dr. N. Biswas
Geophysical Institute
University of Alaska
Fairbanks, AK 99701

Dr. G.A. Bollinger
Department of Geological Sciences
Virginia Polytechnical Institute
21044 Derring Hall
Blacksburg, VA 24061

Dr. Stephen Bratt
Center for Seismic Studies
1300 North 17th Street
Suite 1450
Arlington, VA 22209

Michael Browne
Teledyne Geotech
3401 Shiloh Road
Garland, TX 75041

Mr. Roy Burger
1221 Serry Road
Schenectady, NY 12309

Dr. Robert Burridge
Schlumberger-Doll Research Center
Old Quarry Road
Ridgefield, CT 06877

Dr. W. Winston Chan
Teledyne Geotech
314 Montgomery Street
Alexandria, VA 22314-1581

Dr. Theodore Cherry
Science Horizons, Inc.
710 Encinitas Blvd., Suite 200
Encinitas, CA 92024 (2 copies)

Prof. Jon F. Claerbout
Department of Geophysics
Stanford University
Stanford, CA 94305

Prof. Robert W. Clayton
Seismological Laboratory
Division of Geological & Planetary Sciences
California Institute of Technology
Pasadena, CA 91125

Prof. F. A. Dahlen
Geological and Geophysical Sciences
Princeton University
Princeton, NJ 08544-0636

Prof. Adam Dziewonski
Hoffman Laboratory
Harvard University
20 Oxford St
Cambridge, MA 02138

Prof. John Ebel
Department of Geology & Geophysics
Boston College
Chestnut Hill, MA 02167

Eric Fielding
SNEE Hall
INSTOC
Cornell University
Ithaca, NY 14853

Prof. Donald Forsyth
Department of Geological Sciences
Brown University
Providence, RI 02912

Dr. Cliff Frolich
Institute of Geophysics
8701 North Mopac
Austin, TX 78759

Dr. Anthony Gangi
Texas A&M University
Department of Geophysics
College Station, TX 77843

Dr. Freeman Gilbert
IGPP, A-025
Scripps Institute of Oceanography
University of California
La Jolla, CA 92093

Mr. Edward Giller
Pacific Sierra Research Corp.
1401 Wilson Boulevard
Arlington, VA 22209

Dr. Jeffrey W. Given
SAIC
10260 Campus Point Drive
San Diego, CA 92121

Prof. Roy Greenfield
Geosciences Department
403 Deike Building
The Pennsylvania State University
University Park, PA 16802

Dan N. Hagedorn
Battelle
Pacific Northwest Laboratories
Battelle Boulevard
Richland, WA 99352

Dr. James Hannon
Lawrence Livermore National Laboratory
P. O. Box 808
Livermore, CA 94550

Kevin Hutchenson
Department of Earth Sciences
St. Louis University
3507 Laclede
St. Louis, MO 63103

Dr. Hans Israelsson
Center for Seismic Studies
1300 N. 17th Street, Suite 1450
Arlington, VA 22209-2308

Prof. Thomas H. Jordan
Department of Earth, Atmospheric
and Planetary Sciences
Massachusetts Institute of Technology
Cambridge, MA 02139

Robert C. Kemerait
ENSCO, Inc.
445 Pineda Court
Melbourne, FL 32940

William Kikendall
Teledyne Geotech
3401 Shiloh Road
Garland, TX 75041

Prof. Leon Knopoff
University of California
Institute of Geophysics & Planetary Physics
Los Angeles, CA 90024

Prof. L. Timothy Long
School of Geophysical Sciences
Georgia Institute of Technology
Atlanta, GA 30332

Dr. Gary McCartor
Department of Physics
Southern Methodist University
Dallas, TX 75275

Prof. Art McGarr
Mail Stop 977
Geological Survey
345 Middlefield Rd.
Menlo Park, CA 94025

Dr. George Mellman
Sierra Geophysics
11255 Kirkland Way
Kirkland, WA 98033

Prof. John Nabelek
College of Oceanography
Oregon State University
Corvallis, OR 97331

Prof. Geza Nagy
University of California, San Diego
Department of Ames, M.S. B-010
La Jolla, CA 92093

Dr. Keith K. Nakanishi
Lawrence Livermore National Laboratory
L-205
P. O. Box 808
Livermore, CA 94550

Prof. Amos Nur
Department of Geophysics
Stanford University
Stanford, CA 94305

Prof. Jack Oliver
Department of Geology
Cornell University
Ithaca, NY 14850

Dr. Kenneth Olsen
P. O. Box 1273
Linwood, WA 98046-1273

Howard J. Patton
Lawrence Livermore National Laboratory
L-205
P. O. Box 808
Livermore, CA 94550

Prof. Robert Phinney
Geological & Geophysical Sciences
Princeton University
Princeton, NJ 08544-0636

Dr. Paul Pomeroy
Rondout Associates
P.O. Box 224
Stone Ridge, NY 12484

Dr. Jay Pulli
RADIX System, Inc.
2 Taft Court, Suite 203
Rockville, MD 20850

Dr. Norton Rimer
S-CUBED
A Division of Maxwell Laboratory
P.O. Box 1620
La Jolla, CA 92038-1620

Prof. Larry J. Ruff
Department of Geological Sciences
1006 C.C. Little Building
University of Michigan
Ann Arbor, MI 48109-1063

Dr. Richard Sailor
TASC Inc.
55 Walkers Brook Drive
Reading, MA 01867

Dr. Susan Schwartz
Institute of Tectonics
1156 High St.
Santa Cruz, CA 95064

John Sherwin
Teledyne Geotech
3401 Shiloh Road
Garland, TX 75041

Dr. Matthew Sibol
Virginia Tech
Seismological Observatory
4044 Derring Hall
Blacksburg, VA 24061-0420

Dr. Albert Smith
Lawrence Livermore National Laboratory
L-205
P. O. Box 808
Livermore, CA 94550

Prof. Robert Smith
Department of Geophysics
University of Utah
1400 East 2nd South
Salt Lake City, UT 84112

Dr. Stewart W. Smith
Geophysics AK-50
University of Washington
Seattle, WA 98195

Donald L. Springer
Lawrence Livermore National Laboratory
L-205
P. O. Box 808
Livermore, CA 94550

Dr. George Sutton
Rondout Associates
P.O. Box 224
Stone Ridge, NY 12484

Prof. L. Sykes
Lamont-Doherty Geological Observatory
of Columbia University
Palisades, NY 10964

Prof. Pradeep Talwani
Department of Geological Sciences
University of South Carolina
Columbia, SC 29208

Dr. David Taylor
ENSCO, Inc.
445 Pineda Court
Melbourne, FL 32940

Dr. Steven R. Taylor
Lawrence Livermore National Laboratory
L-205
P. O. Box 808
Livermore, CA 94550

Professor Ta-Liang Teng
Center for Earth Sciences
University of Southern California
University Park
Los Angeles, CA 90089-0741

Dr. R.B. Tittmann
Rockwell International Science Center
1049 Camino Dos Rios
P.O. Box 1085
Thousand Oaks, CA 91360

Dr. Gregory van der Vink
IRIS, Inc.
1616 North Fort Myer Drive
Suite 1440
Arlington, VA 22209

Professor Daniel Walker
University of Hawaii
Institute of Geophysics
Honolulu, HI 96822

William R. Walter
Seismological Laboratory
University of Nevada
Reno, NV 89557

Dr. Gregory Wojcik
Weidlinger Associates
4410 El Camino Real
Suite 110
Los Altos, CA 94022

Prof. John H. Woodhouse
Hoffman Laboratory
Harvard University
20 Oxford St.
Cambridge, MA 02138

Prof. Francis T. Wu
Department of Geological Sciences
State University of New York
at Binghamton
Vestal, NY 13901

Dr. Gregory B. Young
ENSCO, Inc.
5400 Port Royal Road
Springfield, VA 22151-2388

Dr. Eileen Vergino
Lawrence Livermore National Laboratory
L-205
P. O. Box 808
Livermore, CA 94550

J. J. Zucca
Lawrence Livermore National Laboratory
P. O. Box 808
Livermore, CA 94550

Dr. Ralph Alewine III
DARPA/NMRO
1400 Wilson Boulevard
Arlington, VA 22209-2308

Mr. James C. Battis
GL/LWH
Hanscom AFB, MA 01731-5000

Dr. Robert Blandford
AFTAC/CSS
1300 North 17th St., Suite 1450
Arlington, VA 22209-2308

Eric Chael
Division 9241
Sandia Laboratory
Albuquerque, NM 87185

Dr. John J. Cipar
GL/LWH
Hanscom AFB, MA 01731-5000

Cecil Davis
Group P-15, Mail Stop D406
P.O. Box 1663
Los Alamos National Laboratory
Los Alamos, NM 87544

Mr. Jeff Duncan
Office of Congressman Markey
2133 Rayburn House Bldg.
Washington, DC 20515

Dr. Jack Evernden
USGS - Earthquake Studies
345 Middlefield Road
Menlo Park, CA 94025

Art Frankel
USGS
922 National Center
Reston, VA 22092

Dr. Dale Glover
DIA/DT-1B
Washington, DC 20301

Dr. T. Hanks
USGS
Nat'l Earthquake Research Center
345 Middlefield Road
Menlo Park, CA 94025

Paul Johnson
ESS-4, Mail Stop J979
Los Alamos National Laboratory
Los Alamos, NM 87545

Janet Johnston
GL/LWH
Hanscom AFB, MA 01731-5000

Dr. Katharine Kadinsky-Cade
GL/LWH
Hanscom AFB, MA 01731-5000

Ms. Ann Kerr
IGPP, A-025
Scripps Institute of Oceanography
University of California, San Diego
La Jolla, CA 92093

Dr. Max Koontz
US Dept of Energy/DP 5
Forrestal Building
1000 Independence Avenue
Washington, DC 20585

Dr. W.H.K. Lee
Office of Earthquakes, Volcanoes,
& Engineering
345 Middlefield Road
Menlo Park, CA 94025

Dr. William Leith
U.S. Geological Survey
Mail Stop 928
Reston, VA 22092

Dr. Richard Lewis
Director, Earthquake Engineering & Geophysics
U.S. Army Corps of Engineers
Box 631
Vicksburg, MS 39180

James F. Lewkowicz
GL/LWH
Hanscom AFB, MA 01731-5000

Mr. Alfred Lieberman
ACDA/VI-OA'State Department Bldg
Room 5726
320 - 21st Street, NW
Washington, DC 20451

Stephen Mangino
GL/LWH
Hanscom AFB, MA 01731-5000

Dr. Robert Masse
Box 25046, Mail Stop 967
Denver Federal Center
Denver, CO 80225

Art McGarr
U.S. Geological Survey, MS-977
345 Middlefield Road
Menlo Park, CA 94025

Richard Morrow
ACDA/VI, Room 5741
320 21st Street N.W
Washington, DC 20451

Dr. Carl Newton
Los Alamos National Laboratory
P.O. Box 1663
Mail Stop C335, Group ESS-3
Los Alamos, NM 87545

Dr. Kenneth H. Olsen
Los Alamos Scientific Laboratory
P. O. Box 1663
Mail Stop D-406
Los Alamos, NM 87545

Mr. Chris Paine
Office of Senator Kennedy
SR 315
United States Senate
Washington, DC 20510

Colonel Jerry J. Perrizo
AFOSR/NP, Building 410
Bolling AFB
Washington, DC 20332-6448

Dr. Frank F. Pilotte
HQ AFTAC/TT
Patrick AFB, FL 32925-6001

Katie Poley
CIA-OSWR/NED
Washington, DC 20505

Mr. Jack Rachlin
U.S. Geological Survey
Geology, Rm 3 C136
Mail Stop 928 National Center
Reston, VA 22092

Dr. Robert Reinke
WL/NTESG
Kirtland AFB, NM 87117-6008

Dr. Byron Ristvet
HQ DNA, Nevada Operations Office
Attn: NVCG
P.O. Box 98539
Las Vegas, NV 89193

Dr. George Rothe
HQ AFTAC/TTR
Patrick AFB, FL 32925-6001

Dr. Alan S. Ryall, Jr.
DARPA/NMRO
1400 Wilson Boulevard
Arlington, VA 22209-2308

Dr. Michael Shore
Defense Nuclear Agency/SPSS
6801 Telegraph Road
Alexandria, VA 22310

Mr. Charles L. Taylor
GL/LWG
Hanscom AFB, MA 01731-5000

Dr. Larry Turnbull
CIA-OSWR/NED
Washington, DC 20505

Dr. Thomas Weaver
Los Alamos National Laboratory
P.O. Box 1663, Mail Stop C335
Los Alamos, NM 87545

GL/SULL
Research Library
Hanscom AFB , MA 01731-5000 (2 copies)

Secretary of the Air Force
(SAFRD)
Washington, DC 20330

Office of the Secretary Defense
DDR & E
Washington, DC 20330

HQ DNA
Attn: Technical Library
Washington, DC 20305

DARPA/RMO/RETRIEVAL
1400 Wilson Boulevard
Arlington, VA 22209

DARPA/RMO/Security Office
1400 Wilson Boulevard
Arlington, VA 22209

Geophysics Laboratory
Attn: XO
Hanscom AFB, MA 01731-5000

Geophysics Laboratory
Attn: LW
Hanscom AFB, MA 01731-5000

DARPA/PM
1400 Wilson Boulevard
Arlington, VA 22209

Defense Technical Information Center
Cameron Station
Alexandria, VA 22314 (5 copies)

Defense Intelligence Agency
Directorate for Scientific
& Technical IntelligenceAttn: DT1B
Washington, DC 20340-6158

AFTAC/CA
(STINFO)
Patrick AFB, FL 32925-6001

TACTEC
Battelle Memorial Institute
505 King Avenue
Columbus, OH 43201 (Final Report Only)

CONTRACTORS (Foreign)

Dr. Ramon Cabre, S.J.
Observatorio San Calixto
Casilla 5939
La Paz, Bolivia

Prof. Hans-Peter Harjes
Institute for Geophysik
Ruhr University/Bochum
P.O. Box 102148
4630 Bochum 1, FRG

Prof. Eystein Husebye
NTNF/NORSAR
P.O. Box 51
N-2007 Kjeller, NORWAY

Prof. Brian L.N. Kennett
Research School of Earth Sciences
Institute of Advanced Studies
G.P.O Box 4
Canberra 2601, AUSTRALIA

Dr. Bernard Massinon
Societe Radiomana
27 rue Claude Bernard
75005 Paris, FRANCE (2 Copies)

Dr. Pierre Mechler
Societe Radiomana
27 rue Claude Bernard
75005 Paris, FRANCE

Dr. Svein Mykkeltveit
NTNF/NORSAR
P.O. Box 51
N-2007 Kjeller, NORWAY

FOREIGN (Others)

Dr. Peter Basham
Earth Physics Branch
Geological Survey of Canada
1 Observatory Crescent
Ottawa, Ontario, CANADA K1A 0Y3

Dr. Eduard Berg
Institute of Geophysics
University of Hawaii
Honolulu, HI 96822

Dr. Michel Bouchon
I.R.I.G.M.-B.P. 68
38402 St. Martin D'Heres
Cedex, FRANCE

Dr. Hilmar Bungum
NTNF/NORSAR
P.O. Box 51
N-2007 Kjeller, NORWAY

Dr. Michel Campillo
Observatoire de Grenoble
I.R.I.G.M.-B.P. 53
38041 Grenoble, FRANCE

Dr. Kin Yip Chun
Geophysics Division
Physics Department
University of Toronto
Ontario, CANADA M5S 1A7

Dr. Alan Douglas
Ministry of Defense
Blacknest, Brimpton
Reading RG7-4RS, UNITED KINGDOM

Dr. Roger Hansen
NTNF/NORSAR
P.O. Box 51
N-2007 Kjeller, NORWAY

Dr. Manfred Henger
Federal Institute for Geosciences & Nat'l Res.
Postfach 510153
D-3000 Hanover 51, FRG

Ms. Eva Johannisson
Senior Research Officer
National Defense Research Inst.
P.O. Box 27322
S-102 54 Stockholm, SWEDEN

Dr. Fekadu Kebede
Seismological Section
Box 12019
S-750 Uppsala, SWEDEN

Dr. Tormod Kvaerna
NTNF/NORSAR
P.O. Box 51
N-2007 Kjeller, NORWAY

Dr. Peter Marshal
Procurement Executive
Ministry of Defense
Blacknest, Brimpton
Reading FG7-4RS, UNITED KINGDOM

Prof. Ari Ben-Menahem
Department of Applied Mathematics
Weizman Institute of Science
Rehovot, ISRAEL 951729

Dr. Robert North
Geophysics Division
Geological Survey of Canada
1 Observatory Crescent
Ottawa, Ontario, CANADA K1A 0Y3

Dr. Frode Ringdal
NTNF/NORSAR
P.O. Box 51
N-2007 Kjeller, NORWAY

Dr. Jorg Schlittenhardt
Federal Institute for Geosciences & Nat'l Res.
Postfach 510153
D-3000 Hannover 51, FEDERAL REPUBLIC OF GERMANY